การขับเคลื่อนตรงของเครื่องกำเนิดไฟฟ้าชิงโครนัสชนิดหลายขั้วที่ต่อขนานกันหลายตัวสำหรับระบบแปลงผันพลังงานลม

นาย พันไซ จันทวงศ์

ศูนย์วิทยทรัพยากร
จุฬาลงกรณ์มหาวิทยาลัย

วิทยานิพนธ์นี้เป็นส่วนหนึ่งของการศึกษาตามหลักสูตรปริญญาวิศวกรรมศาสตรมหาบัณฑิต
สาขาวิชาวิศวกรรมไฟฟ้า ภาควิชาวิศวกรรมไฟฟ้า
คณะวิศวกรรมศาสตร์ จุฬาลงกรณ์มหาวิทยาลัย
ปีการศึกษา 2553
ลิขสิทธิ์ของจุฬาลงกรณ์มหาวิทยาลัย

A DIRECT DRIVE OF MULTIPLE PARALLEL-CONNECTED MULTI-POLE SYNCHRONOUS GENERATORS FOR WIND ENERGY CONVERSION SYSTEMS

MR. PHANXAY CHANTHAVONG

ศูนย์วิทยทรัพยากร
จุฬาลงกรณ์มหาวิทยาลัย

A Thesis Submitted in Partial Fulfillment of the Requirements
for the Degree of Master of Engineering Program in Electrical Engineering
Department of Electrical Engineering
Faculty of Engineering
Chulalongkorn University
Academic Year 2010
Copyright of Chulalongkorn University

Thesis Title	A DIRECT DRIVE OF MULTIPLE PARALLEL-CONNECTED MULTI-POLE SYNCHRONOUS GENERATORS FOR WIND ENERGY CONVERSION SYSTEMS
By	Mr. Phanxay Chanthavong
Field of Study	Electrical Engineering
Thesis Advisor	Assistant Professor Surapong Suwankawin, Ph. D.
Thesis Co-advisor	Professor Akagi Hirofumi, Ph. D.

Accepted by the Faculty of Engineering, Chulalongkorn University in Partial Fulfillment of the Requirements for the Master's Degree

..... Dean of the Faculty of Engineering
(Associate Professor Boonsom Lerdhirunwong, Dr. Ing.)

THESIS COMMITTEE

..... Chairman
(Associate Professor Youthana Kulvitit, Dr. Ing.)

..... Thesis Advisor
(Assistant Professor Surapong Suwankawin, Ph. D.)

..... Thesis Co-advisor
(Professor Akagi Hirofumi, Ph. D.)

..... Examiner
(Assistant Professor Naebboon Hooncharoen, Ph. D.)

..... External Examiner
(Assistant Professor Nisai Fuengwarodsakul, Dr. Ing.)

พันไช จันทวงศ์ : การขับเคลื่อนตรงของเครื่องกำเนิดไฟฟ้าซิงโครนัสชนิดหลายขั้วที่ต่อขนานกันหลายตัวสำหรับระบบแปลงผันพลังงานลม. (A DIRECT DRIVE OF MULTIPLE PARALLEL-CONNECTED MULTI-POLE SYNCHRONOUS GENERATORS FOR WIND ENERGY CONVERSION SYSTEMS) อ. ที่ปรึกษาวิทยานิพนธ์หลัก : ผู้ช่วยศาสตราจารย์ ดร. สุรพงศ์ สุวรรณกวิน,อ. ที่ปรึกษาวิทยานิพนธ์ร่วม: ศาสตราจารย์ ดร. อคาจิ ฮิโรฟูมิ, 51 หน้า.

เพื่อช่วยลดค่าใช้จ่ายในการลงทุนและส่งเสริมการใช้พลังงานลม วิทยานิพนธ์นี้นำเสนอแนวคิดของเครื่องกำเนิดไฟฟ้าซิงโครนัสแบบต่อเรียงตามกันสำหรับระบบแปลงผันพลังงานลม เครื่องกำเนิดไฟฟ้าซิงโครนัสชนิดแม่เหล็กถาวรหลายขั้วสองตัวจะเชื่อมต่อกันทางกลแบบเรียงตามกัน และ มีการเชื่อมต่อทางไฟฟ้าแบบขนาน โดยอาศัยการควบคุมแบบเวกเตอร์สำหรับการขับเคลื่อนโดยตรง ข้อเสียเปรียบของเครื่องกำเนิดไฟฟ้าแบบต่อเรียงกันคือ ผลกระทบที่เกิดจากพารามิเตอร์ที่ไม่ตรงกันระหว่างเครื่องกำเนิดไฟฟ้า ผลการวิเคราะห์ได้ชี้ให้เห็นว่าผลกระทบจากความไม่ตรงกันของฟลักซ์จะมีนัยสำคัญ ซึ่งทำให้สมรรถนะในการควบคุมแรงบิดลดลง แนวคิดของเครื่องกำเนิดไฟฟ้าแบบต่อเรียงกันสำหรับระบบแปลงผันพลังงานลมได้รับการยืนยันด้วยผลการจำลองการทำงานและผลการทดลอง เครื่องกำเนิดไฟฟ้าแบบต่อเรียงกันที่พัฒนา ขึ้นจะประกอบด้วยเครื่องจักรกลไฟฟ้าชนิดขับเคลื่อนโดยตรงขนาด 300 วัตต์ จำนวน 2 ตัว และ ยังมีส่วนติดตามกำลังงานสูงสุดเพิ่มเติม เข้าไปในส่วนควบคุมของระบบแปลงผันพลังงานลมด้วย ผลการทดสอบแสดงให้เห็นถึงผลสำเร็จในการรวบรวมกำลังงานไฟฟ้าที่ได้จากเครื่องกำเนิดไฟฟ้าแต่ละเครื่อง โดยมีการแบ่งกระแสระหว่างเครื่องกำเนิดไฟฟ้าที่ยอมรับได้

ศูนย์วิทยทรัพยากร
จุฬาลงกรณ์มหาวิทยาลัย

ภาควิชา.....วิศวกรรมไฟฟ้า..... ลายมือชื่อนิสิต.....

สาขาวิชา.....วิศวกรรมไฟฟ้า..... ลายมือชื่อ อ.ที่ปรึกษาวิทยานิพนธ์หลัก.....

ปีการศึกษา 2553 ลายมือชื่อ อ.ที่ปรึกษาวิทยานิพนธ์ร่วม .....

5170666021 : MAJOR ELECTRICAL ENGINEERING
KEYWORDS : DIRECT DRIVE / PMSG / MAXIMUM POWER POINT TRACKING / WIND ENERGY CONVERSION SYSTEMS

PHANXAY CHANTHAVONG : A DIRECT DRIVE OF MULTIPLE MULTI-POLE PARALLEL-CONNECTED MULTI-POLE SYNCHRONOUS GENERATORS FOR WIND ENERGY CONVERSION SYSTEMS .

ADVISOR : ASSISTANT PROFESSOR SURAPONG SUWANKAWIN, Ph. D., CO-ADVISOR : PROFESSOR AKAGI HIROFUMI, Ph. D., 51pp.

To help cut investment cost and encourage the utilization of wind energy, a concept of tandem synchronous generators is proposed for wind energy conversion systems (WECS). Two multi-pole permanent-magnet synchronous generators are mechanically arranged in tandem and electrically connected in parallel and the direct drive can be achieved by using vector control. The drawback of parallel-connected generators is investigated; effects of mismatched parameters are analyzed. It is pointed out that the mismatched flux is considerable and can deteriorate torque controllability. The concept of tandem generators for WECS is verified by simulation and experimental results. The tandem generators are set up with two 350-W direct-drive machines and the maximum power point tracking (MPPT) scheme is additionally included in the developed WECS. The testing results demonstrate the success in gathering electrical power from each generator with tolerable current sharing.

ศูนย์วิทยทรัพยากร
จุฬาลงกรณ์มหาวิทยาลัย

Department : Electrical Engineering Student's Signature .....

Field of Study : Electrical Engineering Advisor's Signature .....

Academic Year : 2010 Co-advisor's Signature .....

ACKNOWLEDGEMENTS

I express, from bottom of heart, my deepest and sincerest appreciation and gratitude to my beloved adviser, Asst. Prof. Dr. Surapong Suwankawin for his instructions, guidance, care, friendly discussion, and continuous encouragement. In my life, I will not forget encouragement and helpful advice for my study at Chulalongkorn University.

I wish to thank my co-advisor: Professor Akagi Hirofumi, for his helpful advice in my research work.

I especially wish to thank my thesis committee: Assoc. Prof. Dr. Youthana Kulvitit, Asst. Prof. Dr. Naebboon Hoonchareon and, Asst. Prof. Dr. Nisai Fuengwarodsakul, for their invaluable advice, thesis supervision, and instructive encouragement.

Unforgettable, I wish to thank Asst. Prof. Dr. Somboon Sengwongwanich for his helpful advice in my live and study at Chulalongkorn University and Mr. Chookiat (APY Engineering Co., Ltd.) for their helpful advice in hardware and implementation.

Thanks also to the lecturers and professors at the Department of Electrical Engineering, Chulalongkorn University, for their invaluable sources of knowledge, and wisdoms.

Very special and profound thanks and gratitude to my beloved parent for their love, constant moral encouragement, and their sacrifice of everything for their sons and daughters. They always support and hold me when I am down so I never lost my spirit. No word I can say about their goodness. I am very proud to be their son. I also thank to my brothers and sister for caring and support. It is to them that I dedicate this thesis.

The last but not least, I would like to express my deepest appreciation to JICA for AUN/SEED-Net project for my financial support, to officers and staffs of International School of Engineering (ISE) and AUN/SEED-Net for their kindness and help during my study.

ศูนย์วิทยทรัพยากร
จุฬาลงกรณ์มหาวิทยาลัย

CONTENTS

ABTRACT [THA] ..... **iv**
ABTRACT [ENG] ..... **v**
ACKNOWLEDGEMENTS ..... **vi**
CONTENTS ..... **vii**
LIST OF FIGURES ..... **ix**
LIST OF TABLES ..... **xii**
LIST OF SYMBOLS ..... **xiii**
LIST OF ABBREVIATIONS ..... **xiv**

CHAPTER I INTRODUCTION **1**
1.1 Small Wind Turbines vs. Tandem Direct-Drive Synchronous Generator 1
1.2 Objective of Research 3
1.3 Scope of Research 3
1.4 Research Methodology 4
1.5 Expected Contribution 4

CHAPTER II TANDEM DIRECT-DRIVE SYNCHRONOUS GENERATORS **5**
2.1 Direct Drive Synchronous Generators 5
2.1.1 Structure and Specification 5
2.1.2 Dynamic Model of PMSG 6
2.2 Tandem Direct-Drive Synchronous Generators with Parallel Connection 7

CHAPTER III CONTROL METHODOLOGY FOR WIND ENERGY CONVERSION SYSTEMS **10**
3.1 Direct Drive of Tandem Synchronous Generators by Vector Control 10
3.2 Maximum Power Point Tracking Scheme 13
3.2.1 Concept of MPPT 13

3.2.2 Power P_e and $\frac{\Delta P_e}{\Delta \omega_m}$ Calculations 14

3.3 Simulation Results 16

3.3.1 Simulation Results of Vector Control System for Tandem Synchronous Generators 16

3.3.2 Simulation Block Diagram of MPPT 17

3.3.3 Wind Turbine Model 18

3.3.4 Simulation Results of Wind Energy Conversion Systems (WECS) 20

CHAPTER IV EFFECTS OF MISMACTHED PARAMETERS 23

4.1 Effects of Mismatched Permanent Magnet Flux, $\Delta\vec{\psi}$ 23

4.2 Effects of Mismatched Stator Resistance, ΔR 29

4.3 Effects of Mismatched Stator Inductance, ΔL 32

4.4 Comparison of Effects of Mismatched Parameters 35

CHAPTER V IMPLEMENTATION AND EXPERIMENTAL RESULTS 36

5.1 Overall experiment setup 36

5.2 Back-to-Back PWM Converter 37

5.3 Wind-Turbine Simulator 37

5.3.1 Wind-turbine simulator by AC drive 37

5.3.2 Evaluation of wind-turbine simulator 38

5.4 Experimental Result of WECS with Tandem Synchronous Generator 40

5.4.1 Performance of MPPT 40

5.4.2 Power gathering and current sharing of tandem generators 41

5.4.3 Effects of mismatched flux position 43

CHAPTER VI CONCLUSIONS 46

6.1 Significant outcomes 46

6.2 Future works 46

REFERENCES 47

APPENDIX 48

BIOGRAPHY 51

LIST OF FIGURES

Figure 1.1 Comparisons of Equipment and Prices 1
Figure 1.2 Tandem Direct-Drive synchronous generators 2
Figure 1.3 Overall wind energy conversion systems 3
Figure 2.1 Local 350-W direct-drive synchronous generator 5
Figure 2.2 Back EMF waveform (from a generator) 5
Figure 2.3 Vector diagram of PMSG and reference frames 6
Figure 2.4 Photo of two synchronous generators is arranged in tandem 7
Figure 2.5 Tandem synchronous generators with parallel connection 8
Figure 2.6 Equivalent circuit of parallel connected synchronous generators 8
Figure 2.7 Resultant equivalent circuits of tandem synchronous generators with parallel connected 9
Figure 3.1 Tandem synchronous generators in wind energy conversion systems 10
Figure 3.2 Vector diagram of vector control for tandem synchronous generators 11
Figure 3.3 Tandem synchronous generators with current feeding 11
Figure 3.4 Vector control feeding 2 multi-poles synchronous generators 12
Figure 3.5 Wind turbine characteristics for various wind speeds 13
Figure 3.6 Block diagram of MPPT methodology 13
Figure 3.7 Power P_e calculation 14
Figure 3.8 Calculation of ΔP_e and $\Delta \omega_m$ 15
Figure 3.9 Calculation of $\frac{\Delta P_e}{\Delta \omega_m}$ 15
Figure 3.10 Simulation block diagram of vector control system 16
Figure 3.11 Simulation results of vector control driving tandem synchronous generators 16
Figure 3.12 Simulation block diagram of MPPT 17
Figure 3.13 Power-speed characteristics of wind turbine 19
Figure 3.14 Block diagram of wind turbine model 19
Figure 3.15 Simulation block diagram of Wind Energy Conversion Systems 20

Figure 3.16 Simulation results showing the performance of MPPT 21
Figure 3.17 Simulation results showing current sharing among generators 22
Figure 3.18 Operation of MPPT on power-speed plane 22
Figure 4.1 Circulating current in tandem generator due to mismatched Parameters 23
Figure 4.2 Vector diagram of mismatched flux and current difference 25
Figure 4.3 Effects of mismatched flux position 26
Figure 4.4 Effects of mismatched flux magnitude 27
Figure 4.5 Simulation results showing the performance of WECS with mismatched flux position 28
Figure 4.6 Vector diagram of current unbalance due to mismatched Parameters 29
Figure 4.7 Current differences $\left|\Delta\vec{i}\right|$ due to mismatched stator resistance, $R_1 = 10.34\ \Omega$ and $R_2 = 8.46\ \Omega$ ($\pm 10\%$ of R) 29
Figure 4.8 Torque unbalance (ΔT_1 and ΔT_2) due to mismatched stator resistance ($R_1 = 10.34\ \Omega$ and $R_2 = 8.46\ \Omega$) 30
Figure 4.9 Simulation results showing the performance of WECS with mismatched stator resistance 31
Figure 4.10 Current differences $\left|\Delta\vec{i}\right|$ due to mismatched stator inductance, $L_1 = 0.0715\ H$ and $L_2 = 0.0585\ H$ ($\pm 10\%$ of L) 32
Figure 4.11 Torque unbalance (ΔT_1 and ΔT_2) due to mismatched stator inductance; $L_1 = 0.0715\ H$ and $L_2 = 0.0585\ H$ ($\pm 10\%$ of L) 33
Figure 4.12 Simulation results showing the performance of WECS with mismatched stator inductance 34
Figure 5.1 Experimental setup of WECS 36
Figure 5.2 Implementation of wind-turbine simulator 38
Figure 5.3 Evaluation of wind-turbine simulator 39
Figure 5.4 Performance of MPPT on power-speed plane when wind speed is varied slowly 40
Figure 5.5 Performance of MPPT on power-speed plane when wind speed is suddenly changed 41

Figure 5.6 Performance of MPPT with single synchronous generators
when wind speed is suddenly changed 41
Figure 5.7 Performance of MPPT with tandem generators when
wind speed is suddenly changed 42
Figure 5.8 Power at grid side 43
Figure 5.9 Back EMF waveforms of tandem synchronous generators 44
Figure 5.10 Experimental results showing current unbalance due to
The effect of mismatched flux position ($\theta = 10°$) 44
Figure 5.11 Simulation results showing current unbalance due to
The effect of mismatched flux position ($\theta = 10°$) 45

ศูนย์วิทยทรัพยากร
จุฬาลงกรณ์มหาวิทยาลัย

LIST OF TABLES

Table 2.1 The rating and specification of PMSG 6
Table 3.1 Parameters of wind turbine characteristics 18
Table 4.1 Comparisons effect of mismatched parameters 35
Table 5.1 Rating of back-to-back PWM converter 37
Table 5.2 Rating of AC servo drive 38

ศูนย์วิทยทรัพยากร
จุฬาลงกรณ์มหาวิทยาลัย

LIST OF SYMBOLS

i_d	Direct-axes current
i_q	Quadrature-axes current
i_{dT}	Total direct-axes current
i_{qT}	Total quadrature-axes current
i_{d1}	Direct-axes current of generator 1
i_{q1}	Quadrature-axes current of generator 1
i_{d2}	Direct-axes current of generator 2
i_{q2}	Quadrature-axes current of generator 2
i_T	Total generator current
i_1	Current of generator 1
i_2	Current of generator 2
v_d	Direct-axes Voltage
v_q	Quadrature-axes Voltage
L	Stator Inductance
R	Stator Resistance
ψ	Rotor Flux
ρ	Rotor Position
p	Number of pole
T	Induced Torque
$P_{WindTurbine}$	Wind Turbine Power
C_p	Power Coefficient
λ	Tip Speed Ratio
β	Blade Pitch Angle
ρ_{Air}	Air Density
R_{Blade}	Blade Length
V_{Wind}	Wind Speed

ศูนย์วิทยทรัพยากร
จุฬาลงกรณ์มหาวิทยาลัย

LIST OF ABBREVIATIONS

SWT	Small Wind Turbine
PMSG	Permanent Magnet Synchronous Generator
PMSM	Permanent Magnet Synchronous Machine
DD	Direct Drive
WECS	Wind Energy Conversion System
MPPT	Maximum Power Point Tracking
AC	Alternating Current
DC	Direct Current
PWM	Pulse Width Modulation
EMF	Electro-Magnetic Force
DSP	Digital Signal Processing
PI	Proportional Integral Controller

ศูนย์วิทยทรัพยากร
จุฬาลงกรณ์มหาวิทยาลัย

CHAPTER I

INTRODUCTION

1.1 Small Wind Turbines vs. Tandem Direct-Drive Synchronous Generators

Wind energy conversion system is one of the most emerging renewable energy technologies. It covers the wide range of power production; with a few tens of kW to multi-MW size wind turbines, and tends to be a mainstream of the electrical power production in several countries. In Thailand, it is, though, in the state of feasibility study for employing the wind energy as an alternative energy source, some small-scaled wind turbine systems have been installed increasingly in some areas. On the other hand, in Laos, the electricity generation is mainly the conventional hydro power plant. However, the concept of wind energy conversion technique can be indirectly adapted for the small hydro power generation in the near future.

Regarding low and medium wind speeds in the Southeast Asia region, the small wind turbines seem to be the appropriate technology. The small wind turbines (SWTs) range from a few watts up to 100 kW, which includes the micro SWTs (up to 1 kW), the mini SWTs (up to 10 kW) and the midi SWTs (up to 100 kW) [6]. The technology trends of SWTs are towards the use of multi-pole permanent magnet synchronous generators (PMSGs) with direct drives. The direct-drive (DD) technology can avoid the drawbacks from the utilization of bulky mechanical gearbox in comparison to conventional geared-machine wind turbines.

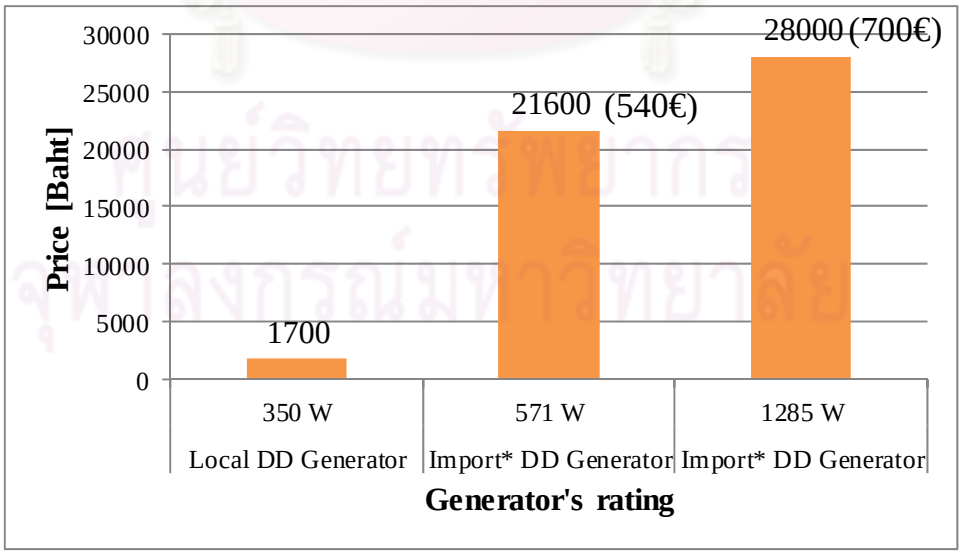

Fig. 1.1 Comparison of PMSG Costs between local and import DD generator.
(* provided by: ALXION Co., Ltd. [France], Exchange rate: 1 € = 40 baht)

Recently, the DD motors are widely used in the home appliances, washing machine for instance. Such motors are the multi-pole synchronous machines which can be suitably applied as the generators for the micro SWTs. Fortunately, as a manufacturing base of home appliances, the low-cost DD machines; as for the spare parts, are widely available in Thailand. Fig. 1.1 provides the comparison of PMSGs costs between the local DD generators and the import DD generators. The figure of Watt/Baht indicates the local DD machine is very much cheaper than the imported ones. Though, the available wattage of local DD generators are quite low (up to 350 W). In order to encourage the utilization of wind energy and to achieve the sustainable development by using the local DD generators, the local DD generators shall be used in tandem as shown in Fig. 1.2. The generators are mechanically coupled on the same shaft, with this driving topology; the larger wattage of DD generators can be obtained. For the investment viewpoint, the using of local DD generators arranged in tandem still gains the benefit; consider a scenario where a 1.2 kW wind turbine system is planned to construct, by comparison with the imported 1.2-kW DD generator, using 4 units of 350-W local DD generator can be 4 times cheaper than that of the former.

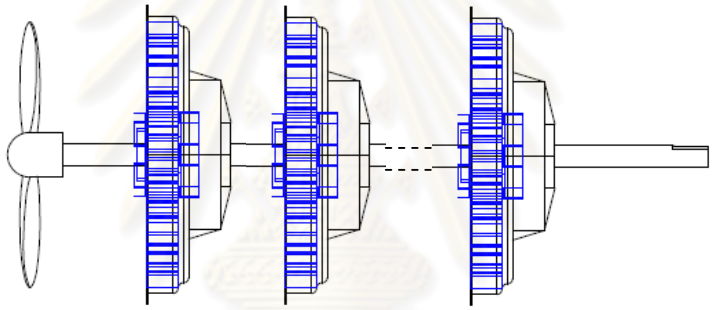

Fig. 1.2 Tandem Direct-Drive synchronous generators.

The literature of multi-electrical-machine drive has mostly been devoted to electric vehicle and railway traction drive applications. Almost all research works have paid attention to induction motor drives. A stator-flux-based vector control is proposed in [1] for the traction drives, a rotor speed of parallel motors shall be selected based on the driving conditions, i.e. acceleration or braking. The main drawback of parallel-connected generators is the circulating current which occurred from the inevitable mismatch of motors' parameters. This circulating current can deteriorate the torque controllability. In [2], the parallel-connected dual induction-motor drive for electric vehicles has been focused. Considering the differences of motor parameters, the electromagnetic torque is expressed in terms of the average total drive torque and the differential torque. In order to effectively control the torque, some suitable reference stator current and rotor flux vectors must be chosen. An adaptive rotor flux observer scheme was introduced in [3] and following the pioneer work in [2], the reference stator current vector is calculated. Subsequent research work in [4] has pointed out the stability problem in the unbalanced-load condition, and the speed regulators are modified to solve this stability obstacle.

In this thesis, the following subjects are conducted:

1) Concerning the driving topology; 2 units of 350 W DD synchronous generators are arranged in tandem, the stator windings are parallelly connected and fed by a back-to-back converter, the overall implementation is shown in Fig. 1.3.
2) Effects of mismatched parameters on the torque controllability are investigated.
3) Maximum-Power-Point-Tracking scheme is created and the performance of the overall system is evaluated by the wind turbine simulator.

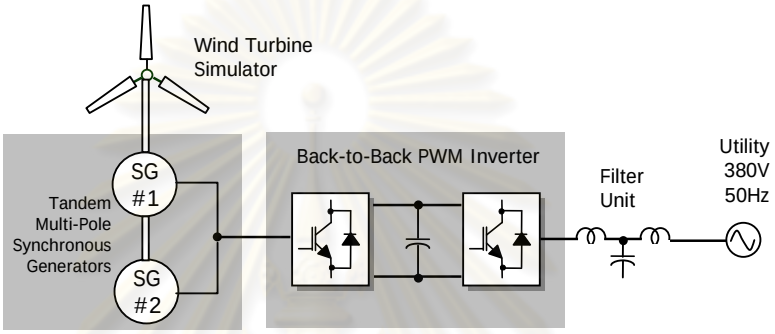

Fig. 1.3 Overall wind energy conversion system

1.2 Objective of Research

The main purpose of the work is devoted to

1. Develop a direct drive of multiple parallel-connected multi-pole permanent-magnet synchronous generators (PMSGs).
2. Investigate the effects on the torque unbalance and torque controllability due to parameter mismatches between 2 generators.
3. Examine the performance of direct drive with the Maximum Power Point Tracking (MPPT) Method on Wind Energy Conversion System (WECS).

1.3 Scope of Research

The scope of this research is limited to

1. Develop a direct drive for 2 parallel-connected multi-pole permanent-magnet synchronous generators (PMSGs) within the power rating of 2x350 W.
2. Sensitivity analysis of generator's parameter mismatches and point out the effects on the torque unbalance and the total torque controllability.
3. Perform the direct drive with the simulated wind turbine system on grid connection.

1.4 Research Methodology

1. Literature reviews of background knowledge relevant to wind energy conversion systems, multi-pole synchronous generators, back-to-back PWM converters and direct-drive concept.
2. Identify salient features of the direct-drive fed wind turbine system.
3. Specify the thesis's objective and the scope of study as appropriate.
4. Develop a direct-drive control scheme for feeding multiple multi-pole synchronous generators.
5. Validate the proposed direct-drive concept of multi-pole synchronous generators with simulations.
6. Construct the wind turbine emulator with AC servo drive and set up all mechanical parts i.e. machine base and mechanical coupling of generators.
7. Implement the direct-drive scheme along with the Back-to-Back PWM converter.
8. Assemble overall system including electrical and mechanical parts.
9. Verify and evaluate the performance of the direct-drive fed wind turbine system.
10. Analyze the experimental results and revise as necessary.
11. Make a conclusion, and write the document for a report and publication.

1.5 Expected Contribution

1. The direct-drive scheme for feeding two multi-pole synchronous generators in wind turbine system.
2. Indicate the drawback of parallel-connected generators due to parameter mismatches.
3. Implementation of low-power wind energy conversion system with proposed direct drive scheme.
4. Grid connection through a back-to-back PWM converter with MPPT algorithm.

ศูนย์วิทยทรัพยากร
จุฬาลงกรณ์มหาวิทยาลัย

CHAPTER II

Tandem Direct-Drive Synchronous Generators

2.1 Direct Drive Synchronous Generators

2.1.1 Structure and specification.

Fig. 2.1 shows physical structure of local DD generator, the rotor is outer type with 48-pole permanent magnet, while the stator winding is concentrated. The back EMF waveform is investigated as shown in Fig. 2.2; sinusoidal back EMF waveform indicates that the generator is the typical Permanent Magnet Synchronous Machine; PMSM. The rating and specification of PMSG are given in Table 2.1.

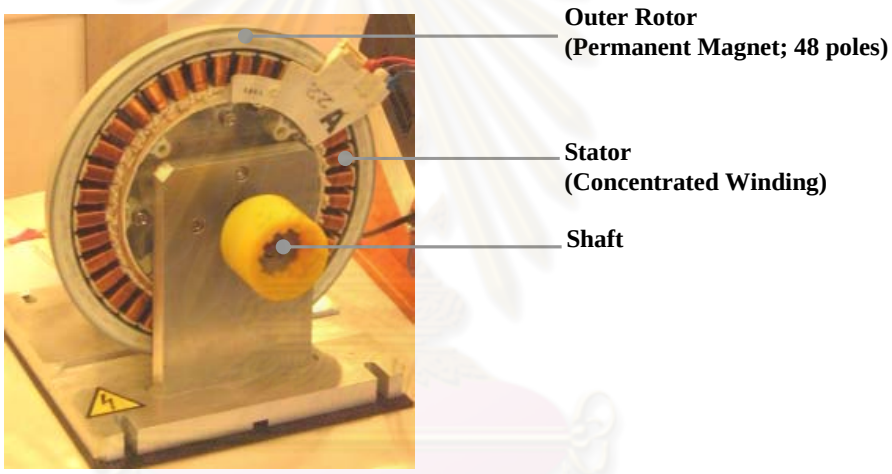

Fig. 2.1 Local 350-W direct-drive synchronous generator.

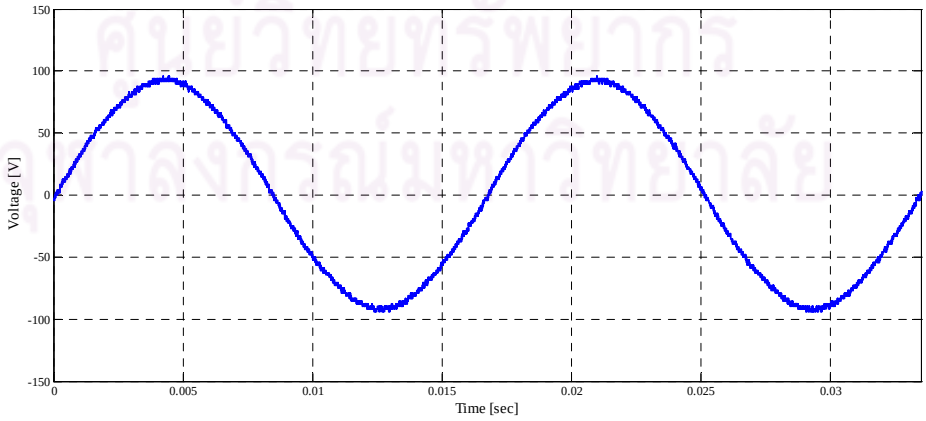

Fig. 2.2 Back EMF waveform (from a generator)

Table 2.1 Rating and specification of PMSG

Parameter	Value	Unit
Stator resistance	9.4	Ω
Stator inductance	65	*mH*
Rotor flux	0.1758	*Wb*
Voltage	220	*V*
Power rating	350	*W*
Number of pole	48	*pole*
Speed	600	*rpm*

2.1.2 Dynamic Model of PMSG

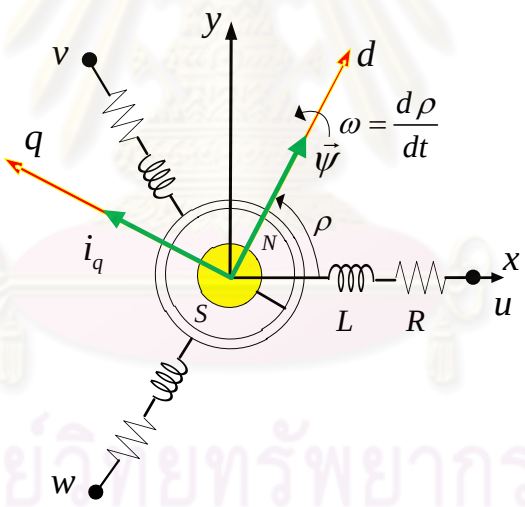

Fig. 2.3 Vector diagram of PMSG on various reference frames.

Dynamic model of a single permanent-magnet-synchronous-generator (PMSG), expressed on the rotating permanent-magnet-flux reference frame; $d-q$ axes, is given in (2.1) – (2.3):

Stator equation:

$$\underbrace{\begin{bmatrix} v_d \\ v_q \end{bmatrix}}_{\vec{v}} = R\underbrace{\begin{bmatrix} i_d \\ i_q \end{bmatrix}}_{\vec{i}} + L\frac{d}{dt}\begin{bmatrix} i_d \\ i_q \end{bmatrix} + \underbrace{\begin{bmatrix} -\omega L i_q \\ \omega L i_d \end{bmatrix}}_{j\omega L\vec{i}} + \underbrace{\begin{bmatrix} 0 \\ \omega\psi \end{bmatrix}}_{j\omega\vec{\psi}} \tag{2.1}$$

Rotor equation:

$$\frac{d}{dt}\begin{bmatrix} \rho \\ \psi \end{bmatrix} = \underbrace{\begin{bmatrix} \omega \\ 0 \end{bmatrix}}_{\vec{\psi}} \tag{2.2}$$

Torque equation:

$$T = \frac{p}{2}\vec{i}\times\vec{\psi} = \frac{p}{2}\cdot i_q \cdot \psi \tag{2.3}$$

2.2 Tandem Direct-Drive Synchronous Generators with Parallel Connection

In this research work, two synchronous generators are arranged in tandem as shown in Fig. 2.4. While the rotor shafts are mechanically coupled, the stator windings are electrically connected in parallel as shown in Fig. 2.5. Fig. 2.6 depicts the equivalent circuit of the parallel connected synchronous generators.

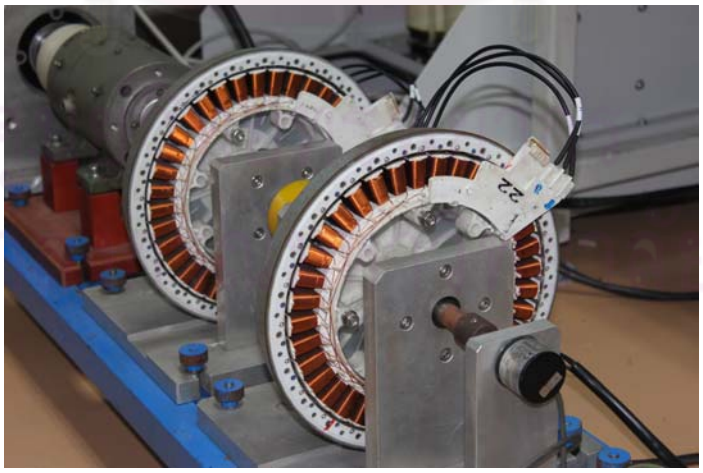

Fig. 2.4 Photo of two synchronous generators arranged in tandem

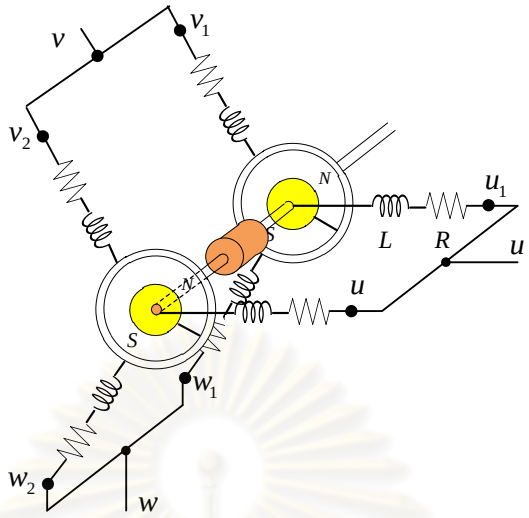

Fig. 2.5 Tandem synchronous generators with parallel connection.

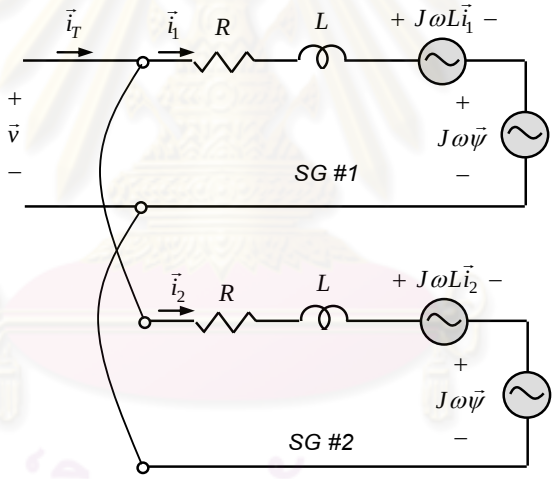

Fig. 2.6 Equivalent circuit of parallel connected synchronous generators.

On the assumption that all parameters of two synchronous generators are definitely equal and both rotor-flux positions are completely aligned, the dynamic model and the resultant equivalent circuit of tandem generators are given in equations (2.4)-(2.6) and Fig. 2.7 respectively.

Stator equation:

$$\begin{bmatrix} v_d \\ v_q \end{bmatrix} = \frac{R}{2}\begin{bmatrix} i_{dT} \\ i_{qT} \end{bmatrix} + \frac{L}{2}\frac{d}{dt}\begin{bmatrix} i_{dT} \\ i_{qT} \end{bmatrix} + \begin{bmatrix} -\omega\frac{L}{2}i_{qT} \\ \omega\frac{L}{2}i_{dT} \end{bmatrix} + \begin{bmatrix} 0 \\ \omega\psi \end{bmatrix} \qquad (2.4)$$

Where $$\vec{i}_T \triangleq \begin{bmatrix} i_{dT} \\ i_{qT} \end{bmatrix} = \begin{bmatrix} i_{d1} \\ i_{q1} \end{bmatrix} + \begin{bmatrix} i_{d2} \\ i_{q2} \end{bmatrix} \triangleq \vec{i}_1 + \vec{i}_2 \qquad (2.5)$$

Total toque equation:

$$T_t = \frac{p}{2}\vec{i}_T \times \vec{\psi} = \frac{p}{2} \cdot i_{qT} \cdot \psi \qquad (2.6)$$

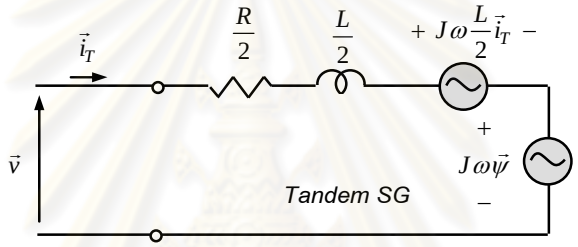

Fig. 2.7 Resultant equivalent circuit of tandem synchronous generators with parallel connected.

It should be noted that, as for the parallel connection of stator windings, the rotor equation for the tandem synchronous generators is as same as that of the single generator in equation (2.2), while the total torque is the summation of the individual ones. Principally, it can be treated with this approach when more than 2 synchronous generators are used in tandem.

ศูนย์วิทยทรัพยากร
จุฬาลงกรณ์มหาวิทยาลัย

CHAPTER III

CONTROL METHODOLOGY FOR WIND ENERGY CONVERSION SYSTEMS

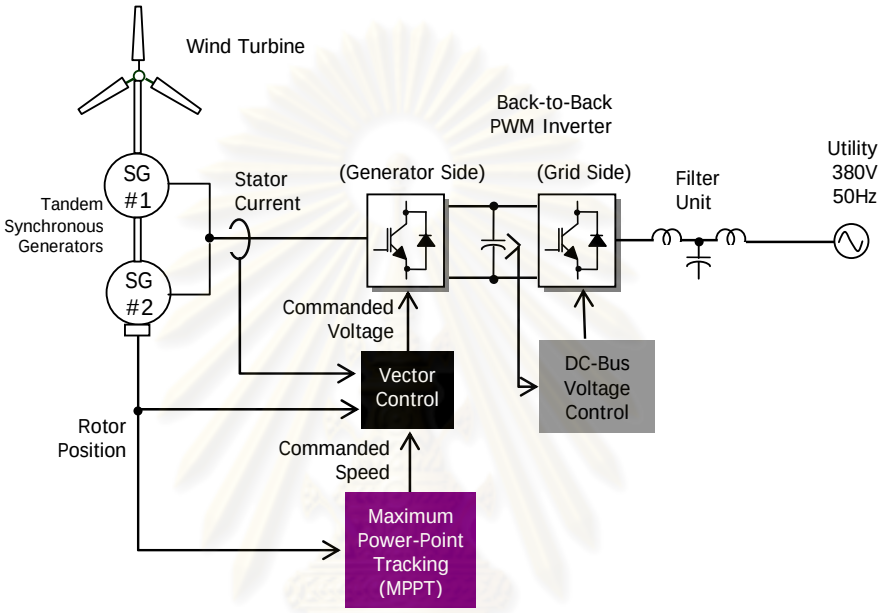

Fig. 3.1 Tandem synchronous generators in wind energy conversion systems.

Fig. 3.1 illustrates the general control structure in wind energy conversion system. The vector control and Maximum Power-Point Tracking (MPPT) scheme are paid attention in this thesis.

3.1 Direct Drive of Tandem Synchronous Generators by Vector Control.

Vector control can directly control the torque, which is well matched with the direct-drive generators. Vector control is based on the knowledge of synchronous generator's model expressed in (2.1)-(2.3). From the torque equation in (2.4), the stator current should be injected in the manner shown in Figs. 3.2 and 3.3. The d-axis current is kept zero ($i_{dT} = i_{d1} = i_{d2} = 0$) in order to obtain the maximum torque per ampere. For the ideal case where all parameters of both generators are identical, the currents are balance:

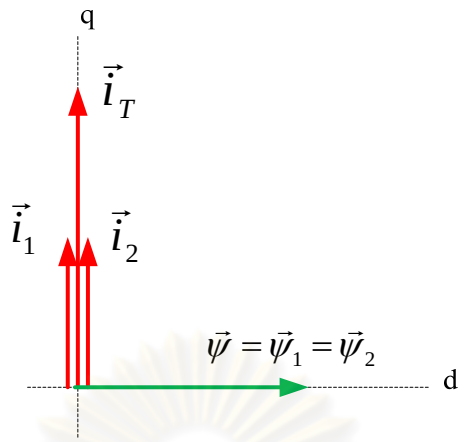

Fig. 3.2 Vector diagram of vector control for tandem synchronous generators.

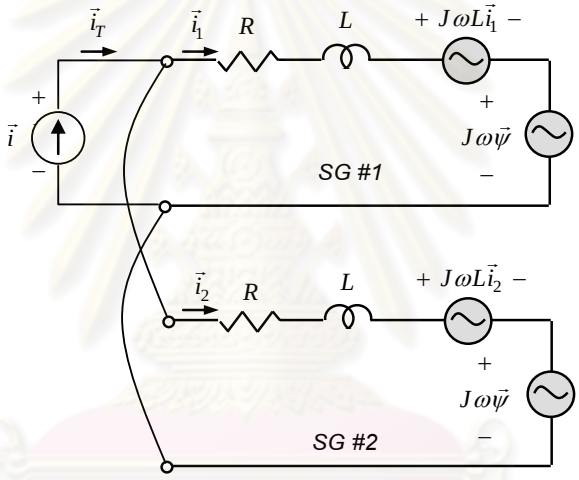

(a) Parallel-connected equivalent circuit,

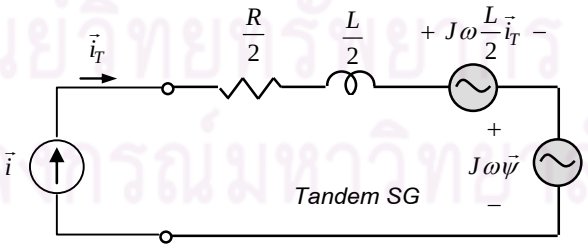

(b) Resultant equivalent circuit.

Fig. 3.3 Tandem synchronous generators with current feeding.

$$\vec{i}_1 = \vec{i}_2 = \frac{\vec{i}_T}{2} \tag{3.1}$$

as well as the induced torques:

$$T_1 = \frac{p}{2}\vec{i}_1 \times \vec{\psi} \tag{3.2}$$

$$T_2 = \frac{p}{2}\vec{i}_2 \times \vec{\psi} \tag{3.3}$$

$$T_1 = T_2 = \frac{p}{2}\frac{\vec{i}_T}{2} \times \vec{\psi} = \frac{p}{2} \cdot \frac{i_{qT}}{2} \cdot \psi . \tag{3.4}$$

And the total torque is:

$$T_t = T_1 + T_2 = \frac{p}{2}\vec{i}_T \times \vec{\psi} = \frac{p}{2} \cdot i_{qT} \cdot \psi \tag{3.5}$$

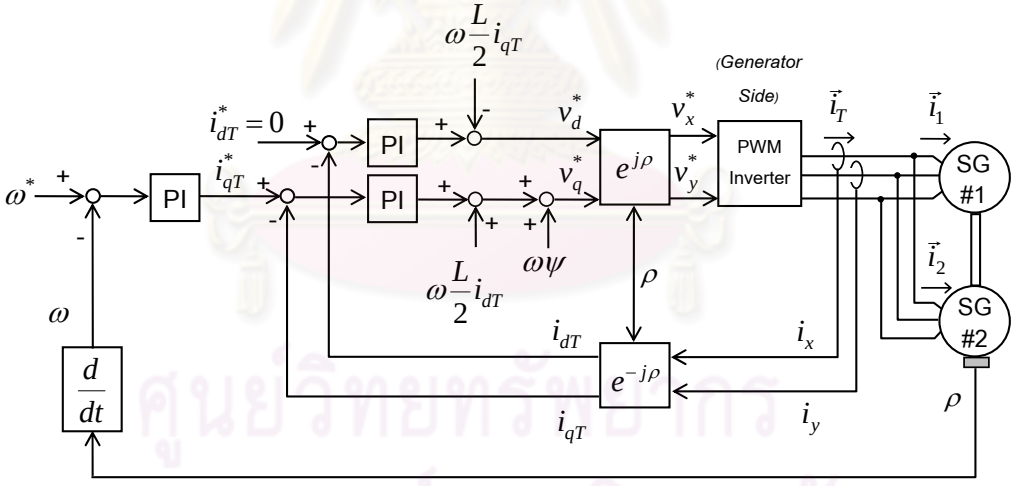

Fig. 3.4 Vector control feeding 2 multi-pole synchronous generators.

Fig. 3.4 shows the block diagram of vector control for the tandem synchronous generators. The inner current control is used to perform as an equivalent current source; the phase currents are measured and transformed to The d,q axes reference frame, with high-bandwidth of current loop, the $d-q$ axes currents can be separately controlled. In order to help the current loop, the feed forward voltage is also added to compensate the cross-coupling induced voltage between the $d-q$ axes. The commanded stator voltage is transformed from $d-q$ axis reference frame to the

stationary frame to be the reference voltage for PWM inverter. The information of flux position is obtained from rotor-position detection with the attached incremental encoder. The outer speed loop is formed for the speed control purpose, i.e. the MPPT scheme that shall be discussed in the next section.

3.2 Maximum-Power-Point-Tracking Scheme

3.2.1 Concept of MPPT

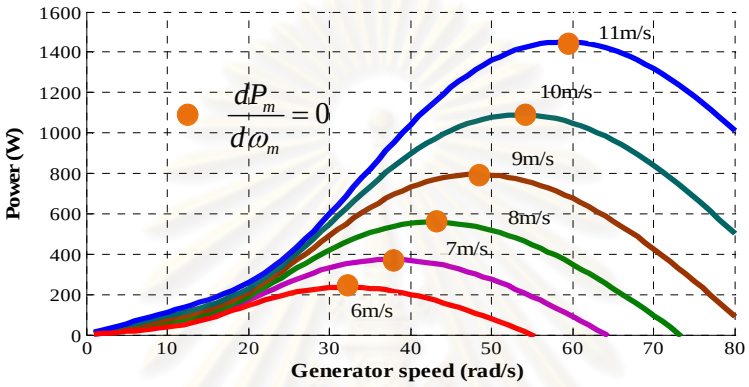

Fig. 3.5 Wind turbine characteristic for various wind speeds.

Generally, the concept of MPPT is created by considering the characteristic of wind turbine as shown in Fig. 3.5. For each wind speed on the power-speed plane, there exists a maximum power point located at a certain rotor speed. And at the maximum power point, the rate of change between power and speed is zero; $\frac{\Delta P_m}{\Delta \omega_m} = 0$. Hence, the MPPT scheme can be conducted in Fig. 3.6.

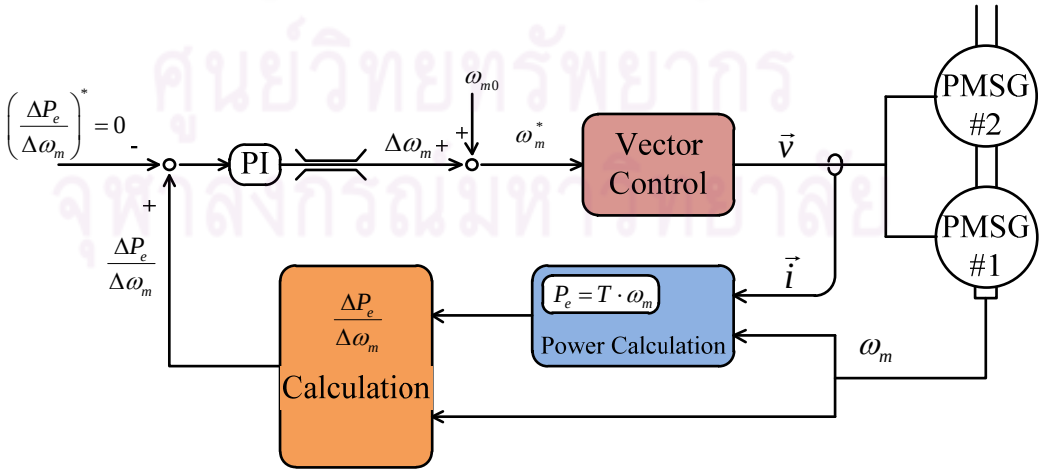

Fig. 3.6 Block diagram of MPPT methodology

Fig. 3.6 shows the direct drive of tandem generators with the MPPT scheme; the vector control and speed control loops described in the previous section are located in the inner loops while the MPPT scheme is at the outer loop. Principally, the mechanism of MPPT is to automatically adjust the generator speed to converge to the optimum one where the generated power is maximized, $\Delta P_e / \Delta \omega_m = 0$. The rate of convergence can be satisfactorily obtained by assigning an appropriate PI gain. Instead of the mechanical power of wind turbine P_m, the electrical power P_e at the generators' terminal is used to manipulate the optimum speed. Beneficially, both copper and core losses of generators are also taken into optimization.

3.2.2 Power P_e and $\frac{\Delta P_e}{\Delta \omega_m}$ calculations

In order to avoid the effect of phase shift of filtered PWM voltage, the electrical power P_e is indirectly obtained from the calculated induced torque. Fig. 3.7 shows the calculation of power P_e, the current $\vec{i}_T$ is detected and, with the information of flux position ρ, the induced torque T_t is carried out. Finally, the electrical power P_e can be obtained by the product of induce torque T_t and generator speed ω_m.

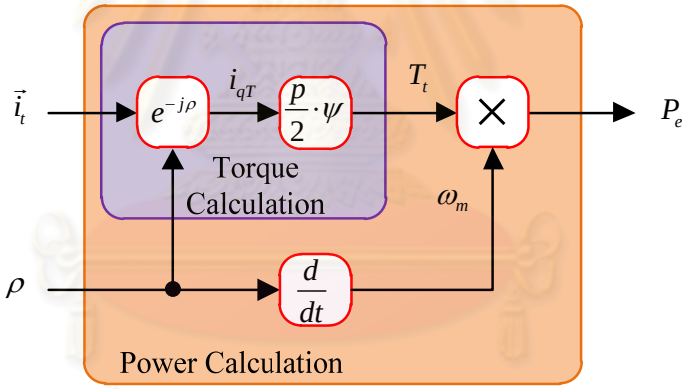

Fig 3.7: Power P_e calculation

The calculation of $\frac{\Delta P_e}{\Delta \omega_m}$ shall be considered in the discrete manner. The deviation of signal can be computed as shown in Fig. 3.8. Using this technique, deviations of both power and speed (ΔP_e and $\Delta \omega_m$) are obtained. Fig. 3.9 depicts the calculation of $\frac{\Delta P_e}{\Delta \omega_m}$ and it is fed back to form the MPPT loop as shown in Fig. 3.6

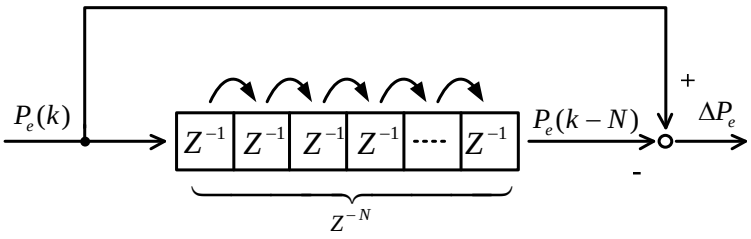

(a) ΔP_e

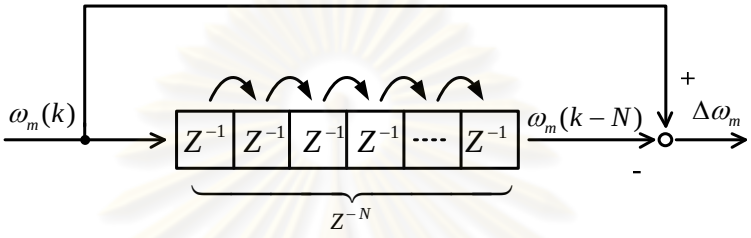

(b) $\Delta \omega_m$

Fig. 3.8 Computation of ΔP_e and $\Delta \omega_m$.

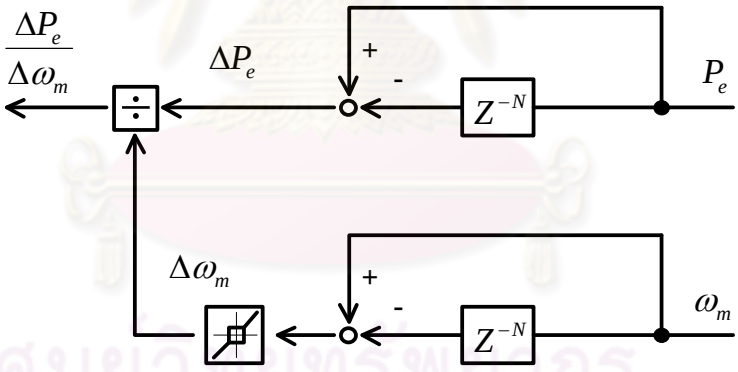

Fig. 3.9 Calculation of $\frac{\Delta P_e}{\Delta \omega_m}$

ศูนย์วิทยทรัพยากร
จุฬาลงกรณ์มหาวิทยาลัย

3.3 Simulation Results

3.3.1 Simulation Results of Vector Control System for Tandem Synchronous Generators.

Fig. 3.10 shows the simulation block diagram of vector control system with two synchronous generators in tandem. At this stage, the speed-loop control is investigated. The performance of vector control is evaluated in Fig. 3.11; the generators' torques can efficiently response against an applied step regenerative load and the speed can be regulated at 40 rad/s. With this ideal case where generators' parameters are matched, the currents and induced torques are equally sharing.

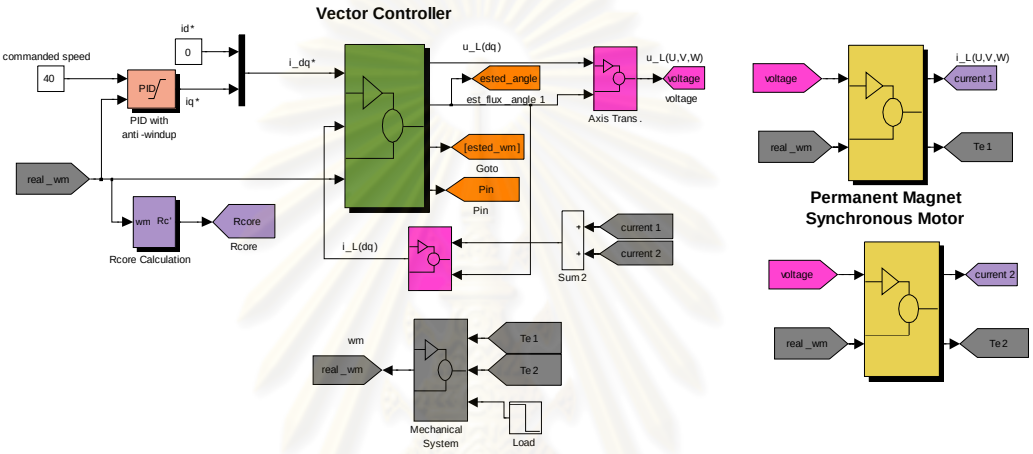

Fig 3.10 Simulation block diagram of vector-control system.

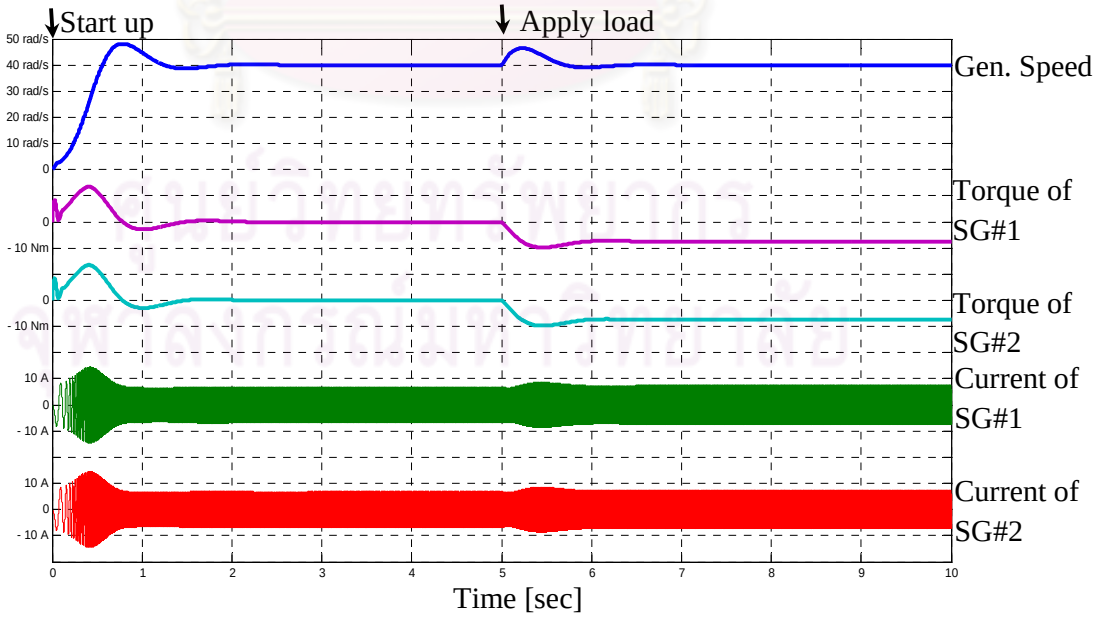

Fig 3.11 Simulation result of vector control driving tandem synchronous generators.

3.3.2 Simulation Block Diagram of MPPT

The simulation block diagram of MPPT scheme is illustrated in Fig. 3.12. It is composed of three parts:

- Power (P_e) calculation in Fig. 3.12 (a),
- $\frac{\Delta P_e}{\Delta \omega_m}$ calculation in Fig. 3.12 (b),
- MPPT loop in Fig. 3.12 (c); a low-pass filter is inserted to obtain the smooth response.

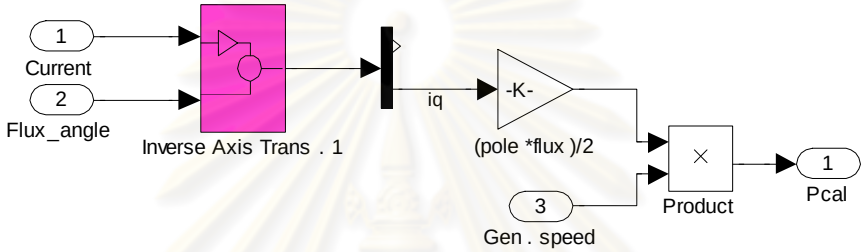

(a) Calculation of P_e

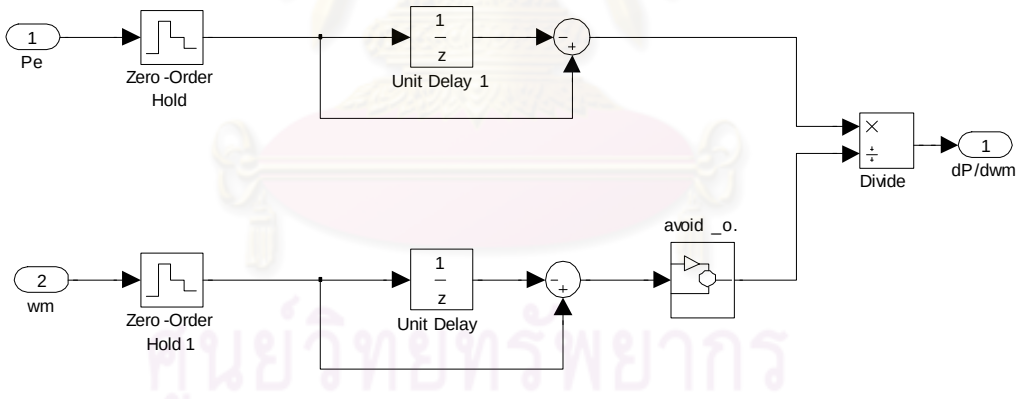

(b) Calculation of $\frac{\Delta P_e}{\Delta \omega_m}$

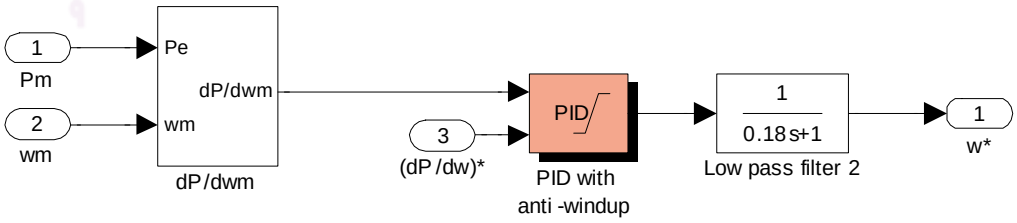

(c) MPPT Block

Fig. 3.12 Simulation block diagram of MPPT.

ศูนย์วิทยทรัพยากร
จุฬาลงกรณ์มหาวิทยาลัย

3.3.3 Wind-Turbine Model.

The wind-turbine model is based on the power-speed characteristics as given in (3.6)

$$P_{WindTurbine} = C_p(\lambda,\beta)\frac{\rho_{Air}\times(\pi R_{Blade}^2)}{2}V_{Wind}^3, \tag{3.6}$$

where the power coefficient $C_p(\lambda,\beta)$ is

$$C_p(\lambda,\beta) = C_1\left(\frac{C_2}{\lambda_i} - C_3\beta - C_4\right)\exp\left(\frac{-C_5}{\lambda_i}\right) + C_6\lambda \tag{3.7}$$

$$\lambda_i = \left[\frac{1}{\lambda + 0.08\beta} - \frac{0.035}{\beta^3 + 1}\right]^{-1} \tag{3.8}$$

$$\lambda = \frac{\omega_m R_{Blade}}{V_{Wind}} \tag{3.9}$$

Table 3.1 Parameters and rating of wind turbine.

WT Power Rating $P_{WindTurbine}$	$800W$	C_1	0.45
Blade Pitch Angle β	$0°$	C_2	90
Air Density ρ_{Air}	$1.184\,kg/m^3$	C_3	0.4
Blade Length R_{Blade}	$1.2m$	C_4	6.9
Wind Speed V_{Wind}	$6-9\,m/s$	C_5	17.3
		C_6	0.0029

Parameters and rating of using wind turbine are specified in Table 3.1. Regarding equations (3.6)-(3.9) and Table 3.1, the power-speed characteristics for various wind speed can be shown in Fig 3.13.

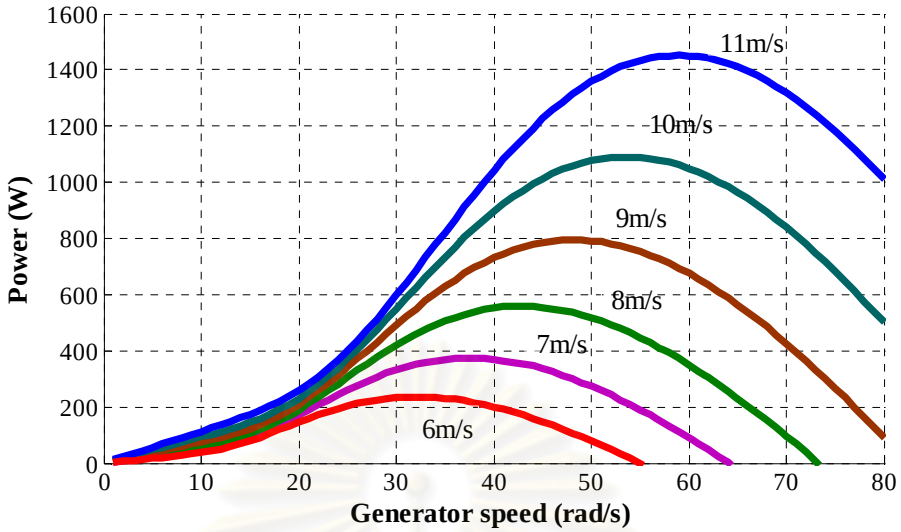

Fig. 3.13 Power-speed characteristics of wind turbine.

From the aforementioned wind turbine characteristic, the model of wind turbine can be created as shown in Fig. 3.14. Wind speed and generator speed are required as inputs, the output is the mechanical torque, T_m , which behaves as a prime mover for generators.

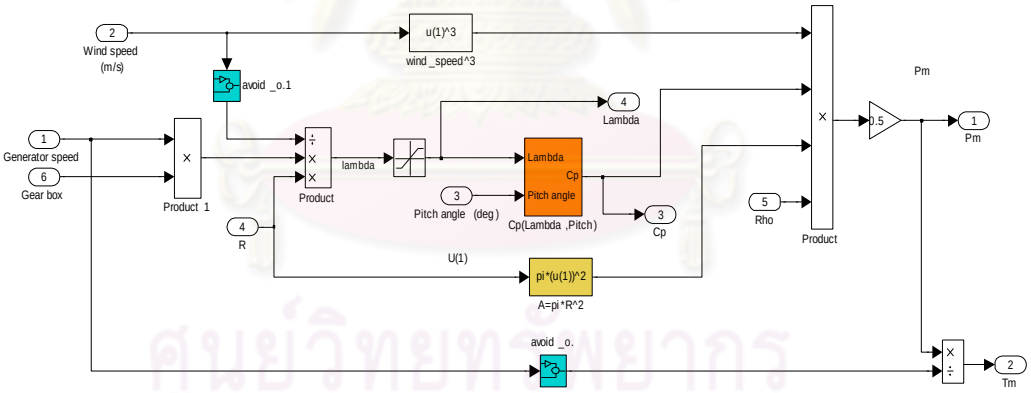

Fig. 3.14 Block diagram of wind-turbine model.

ศูนย์วิทยทรัพยากร
จุฬาลงกรณ์มหาวิทยาลัย

3.3.4 Simulation Results of Wind Energy Conversion Systems (WECS)

By integrating the above block diagram in section 3.3.1-3.3.3, the overall block diagram of WECS can then be obtained in Fig. 3.15. The wind turbine is included as a prime mover of tandem generators and the MPPT is located at the outer loop and provides commanded speed for vector control (direct drive).

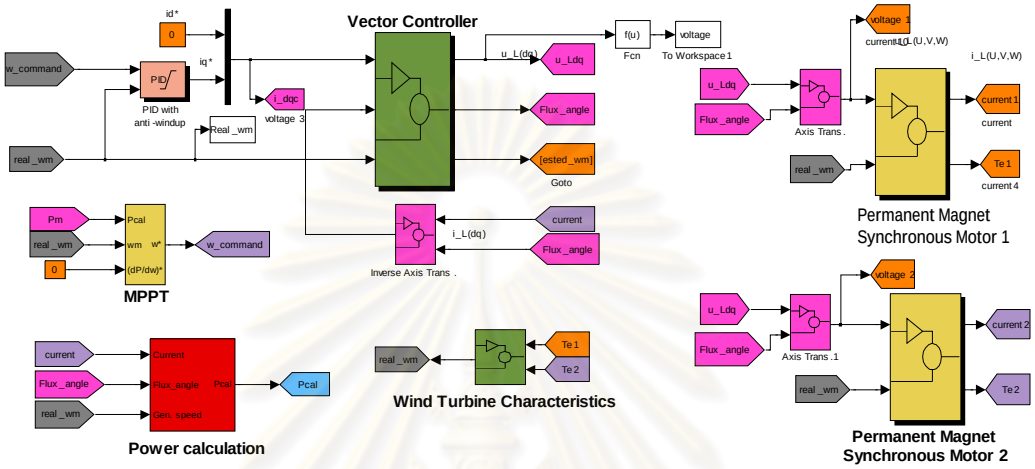

Fig 3.15 Simulation block diagram of Wind Energy Conversion Systems.

The simulation results in Figs. 3.16 and 3.17 show the performance of direct drive for various wind speeds. The generators' torque can be properly controlled during the sudden change of wind speed and the induced torque; also the current, of each generator is finely balanced. The MPPT can successfully track the maximum power point according to each wind speed with acceptable rate of convergence. Fig. 3.18 gives another viewpoint, on the power-speed plane, for the operation of MPPT.

ศูนย์วิทยทรัพยากร
จุฬาลงกรณ์มหาวิทยาลัย

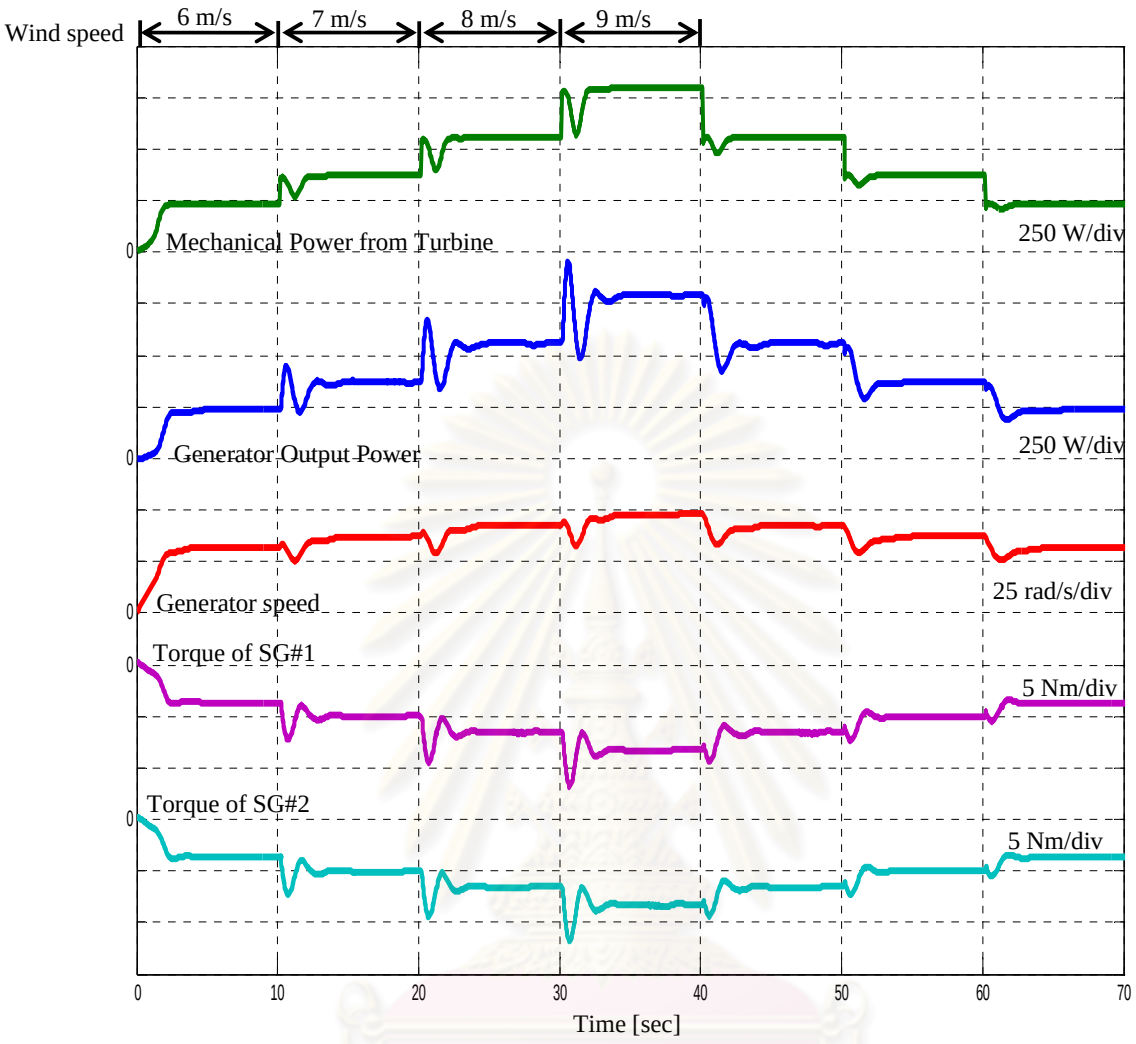

Fig. 3.16 Simulation result showing the performance of MPPT

ศูนย์วิทยทรัพยากร
จุฬาลงกรณ์มหาวิทยาลัย

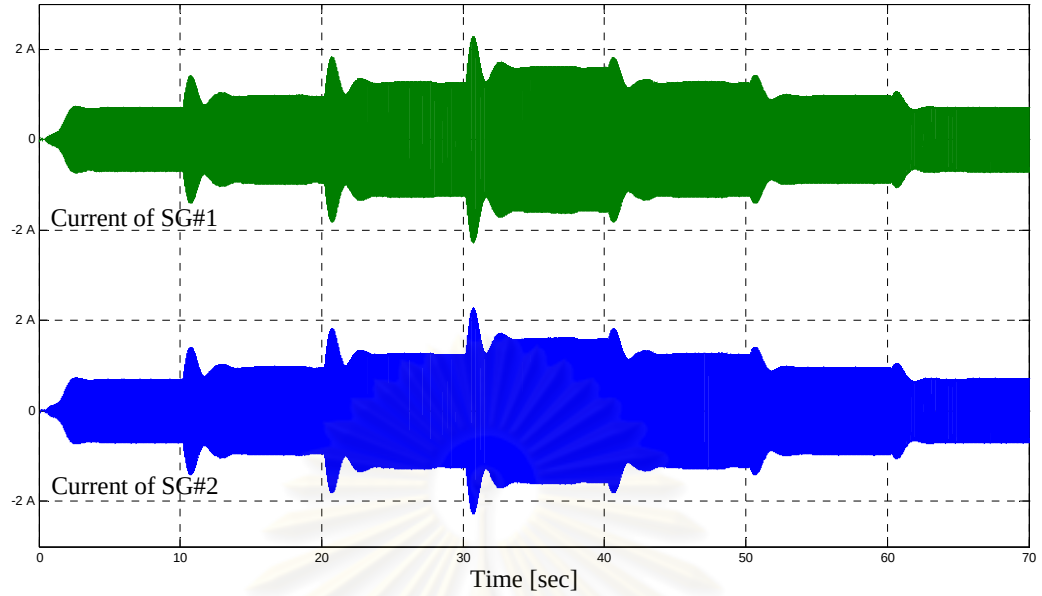

Fig. 3.17 Simulation result showing current sharing among generators.

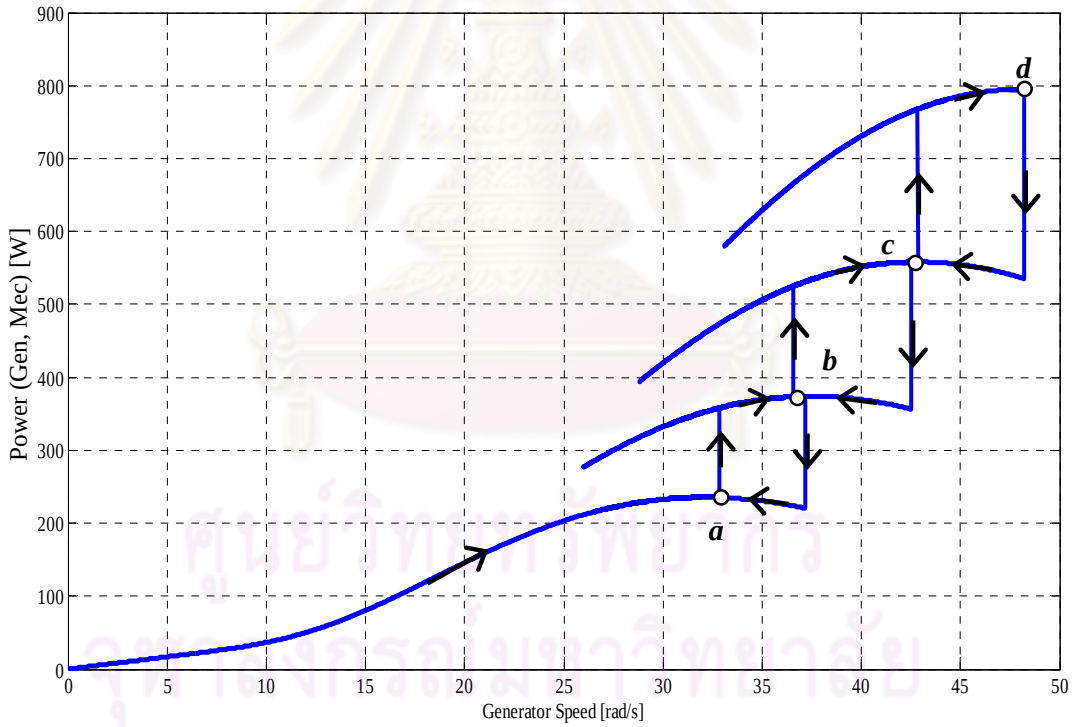

Fig. 3.18 Operation of MPPT on power-speed plane.

CHAPTER IV

EFFECTS OF MISMATCHED PARAMETERS

The main drawback of tandem generators connected in parallel are the effects of mismatched parameters. Once any parameters are mismatched, the current among two generators will be unbalance ($\vec{i}_1 \neq \vec{i}_2$) with the flowing of circulating current as shown by the dash line in Fig. 4.1. The mismatched parameters consequently lead to the torque unbalance between the generators. In the i.e. subsections, the effects of three mismatched parameters shall be investigated, the mismatched of permanent magnet flux, stator resistance and stator inductance.

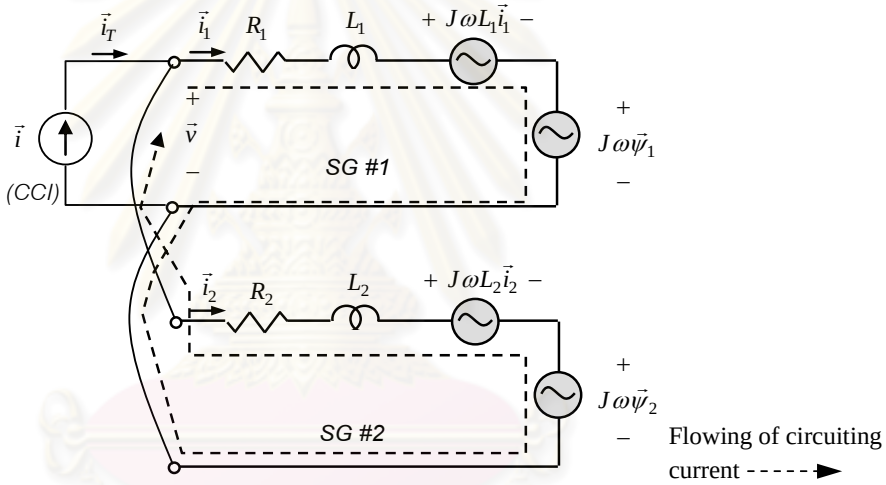

Fig. 4.1 Circulating current in tandem generators due to mismatched parameters.

4.1 Effects of Mismatched Permanent Magnet Flux, $\Delta\vec{\psi}$

The mismatch of flux $\Delta\vec{\psi}$ can be arisen from the variation of flux excitation in the production process and/or the inaccuracy in the mechanical alignment of the zero position of both generators, especially for the multi-pole synchronous generators. From (2.1) and Fig. 4.1, the relationship between the flux mismatch $\Delta\vec{\psi}$ and the current difference $\Delta\vec{i}$ can be derived as:

$$\Delta\vec{i} = -\frac{\omega J}{RI + (sI + \omega J)L} \cdot \Delta\vec{\psi} \qquad (4.1)$$

where

$$\vec{i}_T = \vec{i}_1 + \vec{i}_2 \quad , \quad \Delta\vec{i} = \vec{i}_1 - \vec{i}_2$$

and

$$\vec{\psi} \triangleq \frac{\vec{\psi}_1+\vec{\psi}_2}{2} \quad , \quad \Delta\vec{\psi} = \vec{\psi}_1-\vec{\psi}_2$$

From (4.1), the vector diagram of mismatched flux versus current difference can be drawn in Fig. 4.2. The induced torque for each generator can be written as:

Torque of SG #1:

$$\begin{aligned} T_1 &= \frac{p}{2}\vec{i}_1\times\vec{\psi}_1 \\ &= \frac{p}{2}\left\{\frac{\vec{i}_T}{2}\times\vec{\psi}+\underbrace{\frac{\Delta\vec{i}}{2}\times\vec{\psi}+\frac{\vec{i}_T}{2}\times\frac{\Delta\vec{\psi}}{2}+\frac{\Delta\vec{i}}{2}\times\frac{\Delta\vec{\psi}}{2}}_{\Delta T_1}\right\} \end{aligned} \qquad (4.2)$$

Torque of SG #2:

$$\begin{aligned} T_2 &= \frac{p}{2}\vec{i}_2\times\vec{\psi}_2 \\ &= \frac{p}{2}\left\{\frac{\vec{i}_T}{2}\times\vec{\psi}-\underbrace{\frac{\Delta\vec{i}}{2}\times\vec{\psi}-\frac{\vec{i}_T}{2}\times\frac{\Delta\vec{\psi}}{2}+\frac{\Delta\vec{i}}{2}\times\frac{\Delta\vec{\psi}}{2}}_{\Delta T_2}\right\} \end{aligned} \qquad (4.3)$$

The total induced torque is

$$\begin{aligned} T_t &= T_1+T_2 \\ &= \frac{p}{2}\left\{\vec{i}_T\times\vec{\psi}+\underbrace{\frac{1}{2}\cdot\Delta\vec{i}\times\Delta\vec{\psi}}_{\Delta T}\right\} \end{aligned} \qquad (4.4)$$

It can be observed that the mismatched flux not only causes the torque unbalance between the generators; ΔT_1 and ΔT_2 in (4.2) and (4.3) respectively, but also affects the overall toque controllability of the vector control; ΔT in (4.4). The effects from the mismatched flux will be focused separately on the differences in misalignment of flux position (Fig. 4.3) and flux magnitude (Fig. 4.4). The sensitivities for various operating conditions are investigated by varying the speed ω and current i_q. Figs. 4.3(a) - 4.3(c) depict the current difference ($\left|\Delta\vec{i}\right|$), torque unbalance ($\Delta T_1$ and ΔT_2) and overall torque error (ΔT) due to the flux-position mismatch. From Fig. 4.3(a), in comparison to the low-speed range, the current difference is larger in medium and high speed range, this manner also reflects to the

torque unbalance as shown in Fig. 4.3(b). In contrast to the torque unbalance, the total torque controllability is quite poor in the low-speed range as shown in Fig. 4.3(c).

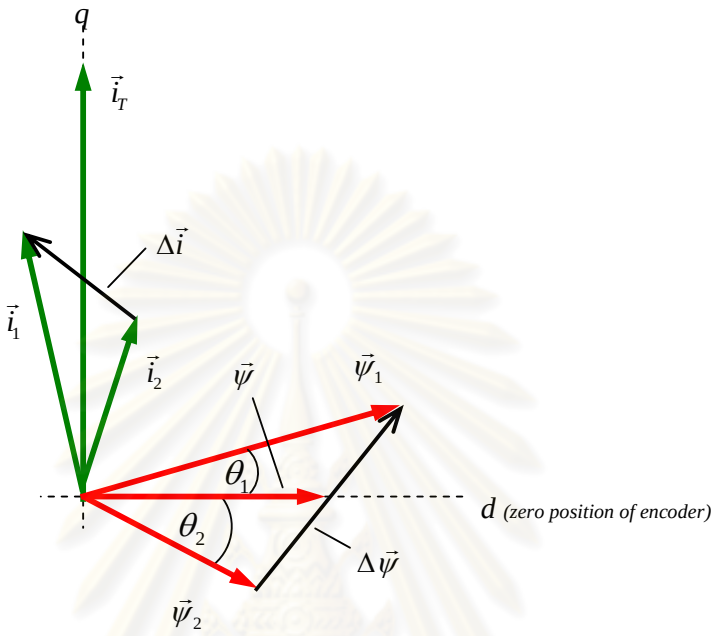

Fig. 4.2 Vector diagram of mismatched flux and current difference.

Effects of mismatched flux magnitude are also given in Figs. 4.4(a)–4.4(c). As pointed out in Fig. 4.4(b), the torque unbalance is varied according to generator's current, while the total torque error, in Fig. 4.4(c) is severe in low-speed range as same as that of the mismatched flux position in Fig. 4.3(c). The overall performance with WECS is evaluated and shown in Fig. 4.5, unbalanced current and torque are varied depending on the generator speed, this agrees well with the analysis in Fig. 4.3(a) and 4.3(b). Nevertheless, the MPPT still works properly. It can be concluded that the unbalanced current and torque are the main effects of mismatched flux, consequently, the utilization of inverters' current rating is degradation.

จุฬาลงกรณ์มหาวิทยาลัย

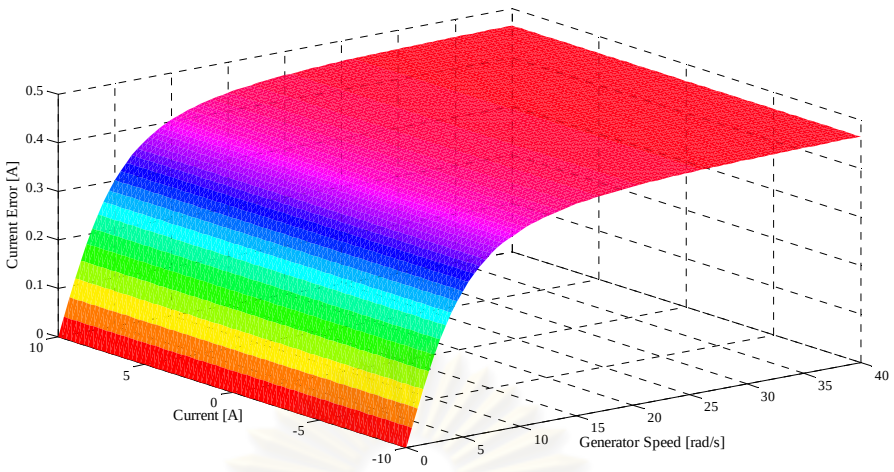

(a) Current difference ($|\Delta\vec{i}|$) due to mismatch of flux position, $\theta_1 = 0$ and $\theta_2 = 10°$.

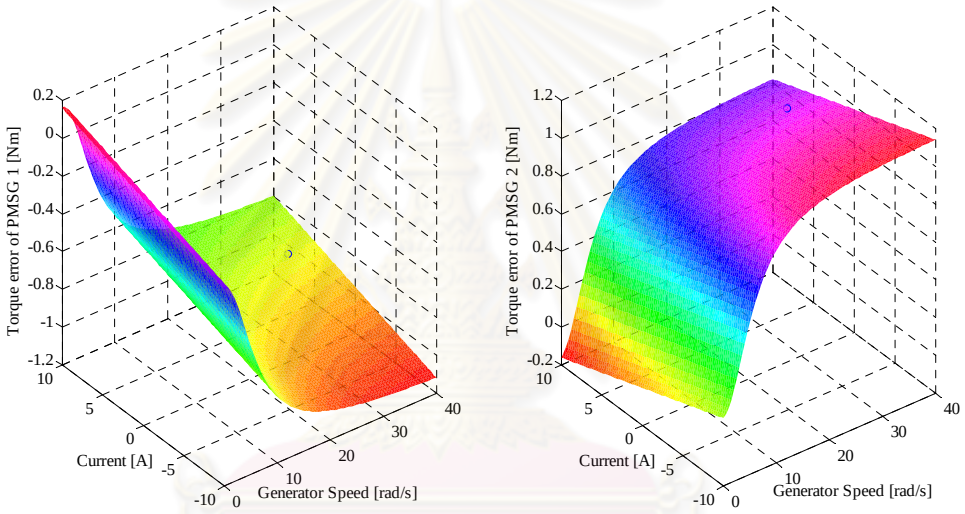

(b) Torque unbalance (ΔT_1 and ΔT_2) due to mismatch of flux position, $\theta_1 = 0°$ and $\theta_2 = 10°$.

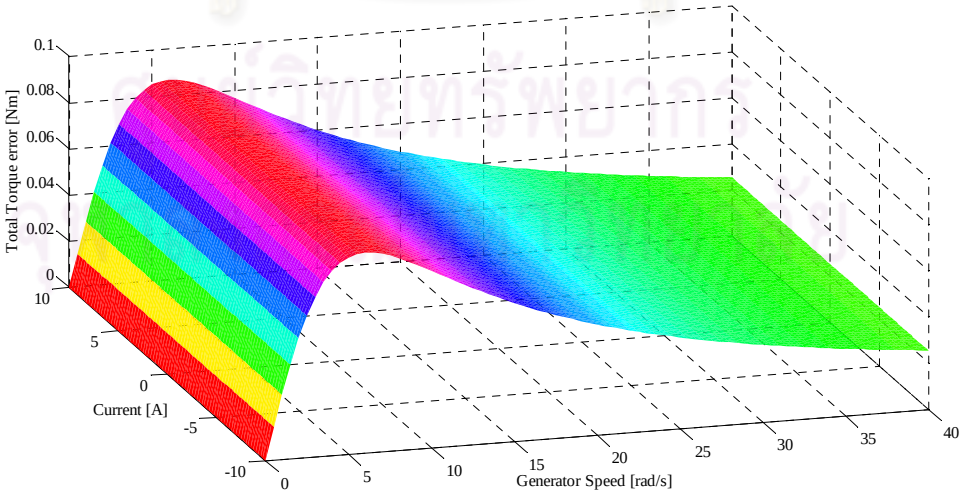

(c) Total torque error, ΔT due to mismatch of flux position, $\theta_1 = 0°$ and $\theta_2 = 10°$.

Fig. 4.3 Effects of mismatched flux position.

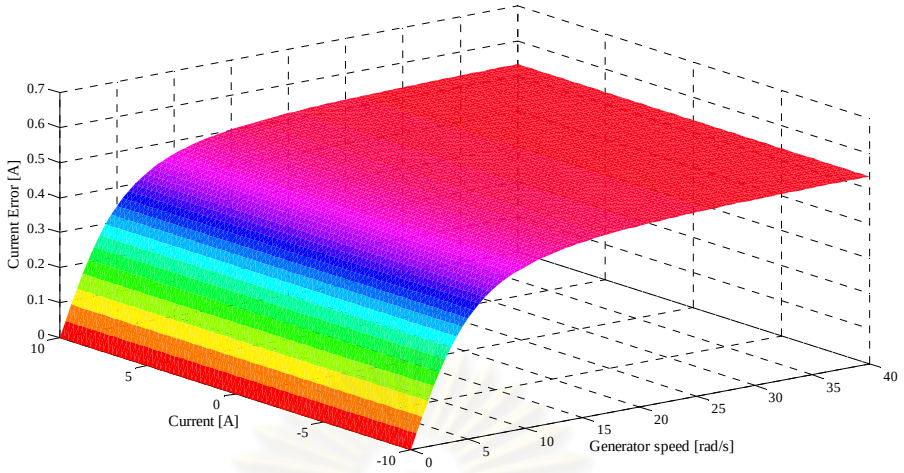

(a) Current difference ($|\Delta\vec{i}|$) due to mismatch of flux amplitude,

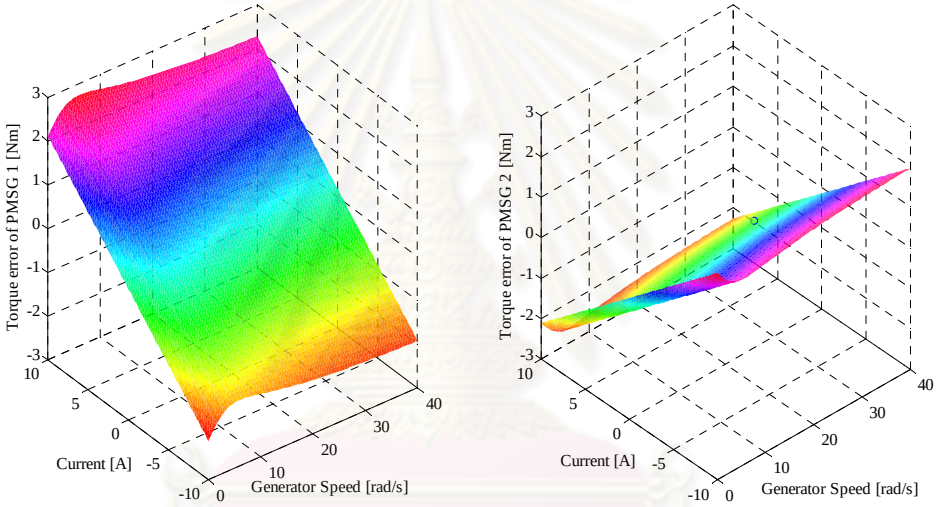

(b) Torque unbalance (ΔT_1 and ΔT_2) due to mismatch of flux amplitude,

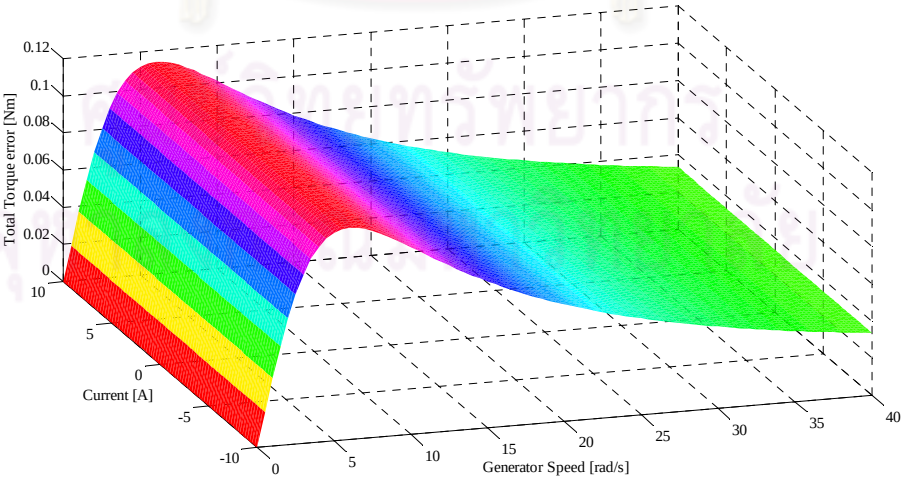

(c) Total torque error, ΔT due to mismatch of flux amplitude.

Fig. 4.4 Effects of mismatched flux magnitude
$\psi_1 = 0.19338$ and $\psi_2 = 0.15822$ ($\pm 10\%$ of $|\psi|$).

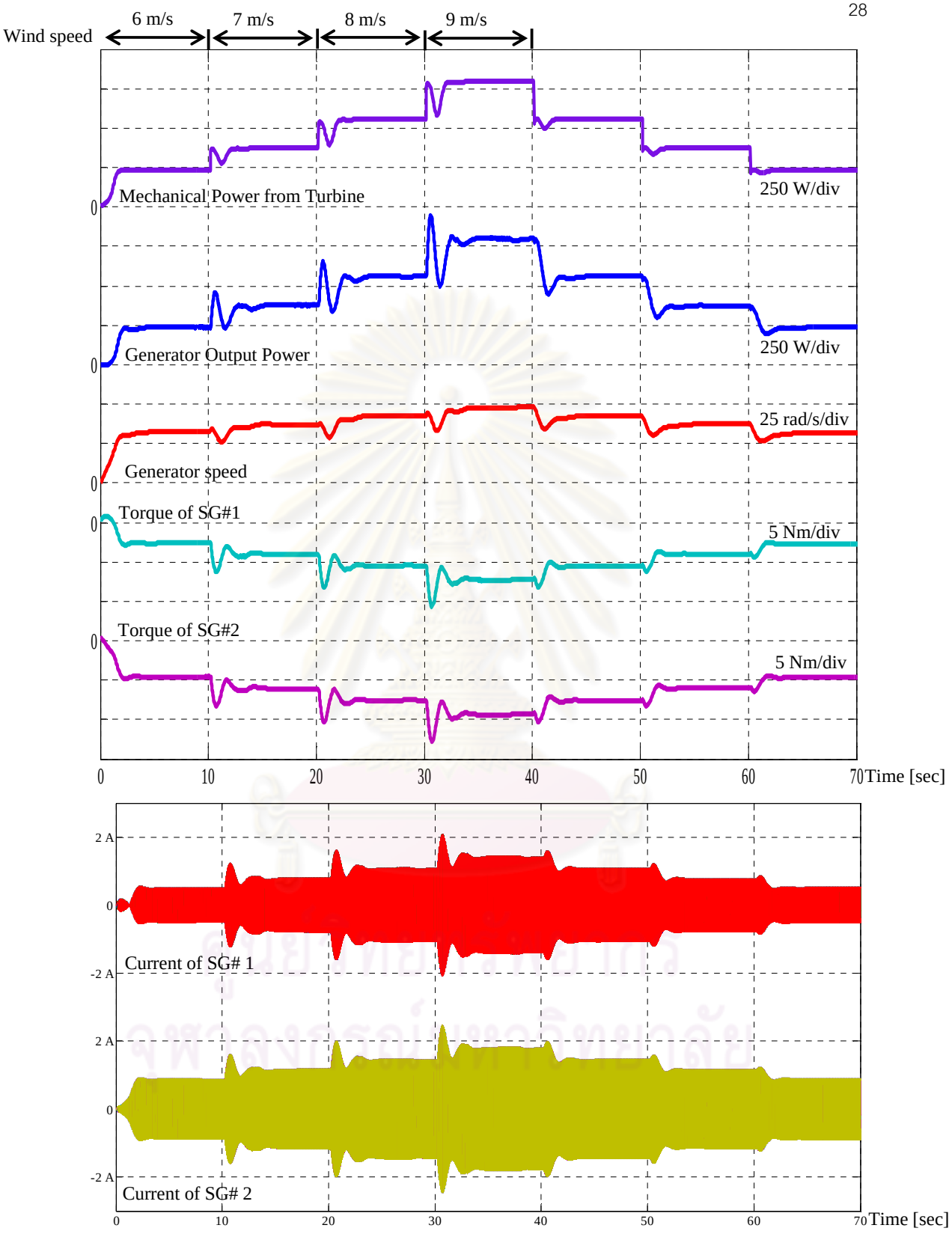

Fig. 4.5 Simulation results showing the performance of WECS with mismatched flux position.

4.2 Effects of Mismatched Stator Resistance ΔR.

From (2.1) and Fig 4.1, the relationship between the mismatched stator resistance and the current difference $\Delta\vec{i}$ can be derived as:

$$\Delta\vec{i} = \frac{(R_2 - R_1)\cdot I}{(R_1 + R_2)I + (sI + \omega J)2L}\cdot\vec{i} \qquad (4.5)$$

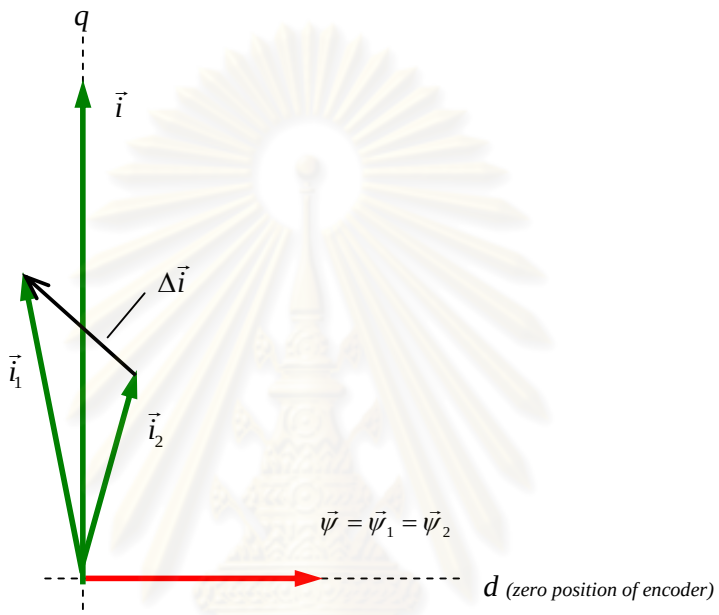

Fig. 4.6 Vector diagram of current unbalance due to mismatched stator resistance.

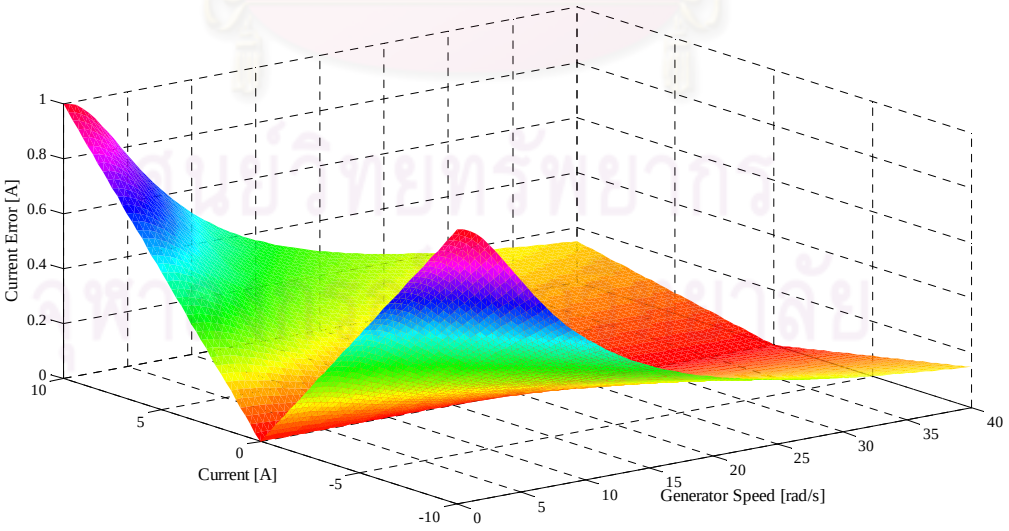

Fig. 4.7 Current differences $|\Delta\vec{i}|$ due to mismatched stator resistance, $R_1 = 10.34\ \Omega$ and $R_2 = 8.46\ \Omega$ ($\pm 10\%$ of R).

From (4.5), the magnitude of current difference is illustrated in Fig 4.7. It is observed that the unbalance current vastly occurred in the low-speed range especially at high current (torque).

From (4.5), the induced torque for each generator can be written as:

Torque of SG #1:

$$T_1 = \frac{p}{2}\vec{i}_1 \times \vec{\psi}_1$$

$$= \frac{p}{2}\left\{\frac{\vec{i}_T}{2} \times \vec{\psi} + \underbrace{\frac{\Delta\vec{i}}{2} \times \vec{\psi}}_{\Delta T_1}\right\} \qquad (4.6)$$

Torque of SG #2:

$$T_2 = \frac{p}{2}\vec{i}_2 \times \vec{\psi}_2$$

$$= \frac{p}{2}\left\{\frac{\vec{i}_T}{2} \times \vec{\psi} - \underbrace{\frac{\Delta\vec{i}}{2} \times \vec{\psi}}_{\Delta T_2}\right\} \qquad (4.7)$$

The total induced torque is

$$T_t = T_1 + T_2$$

$$= \frac{p}{2}\left\{\vec{i}_T \times \vec{\psi}\right\} \qquad (4.8)$$

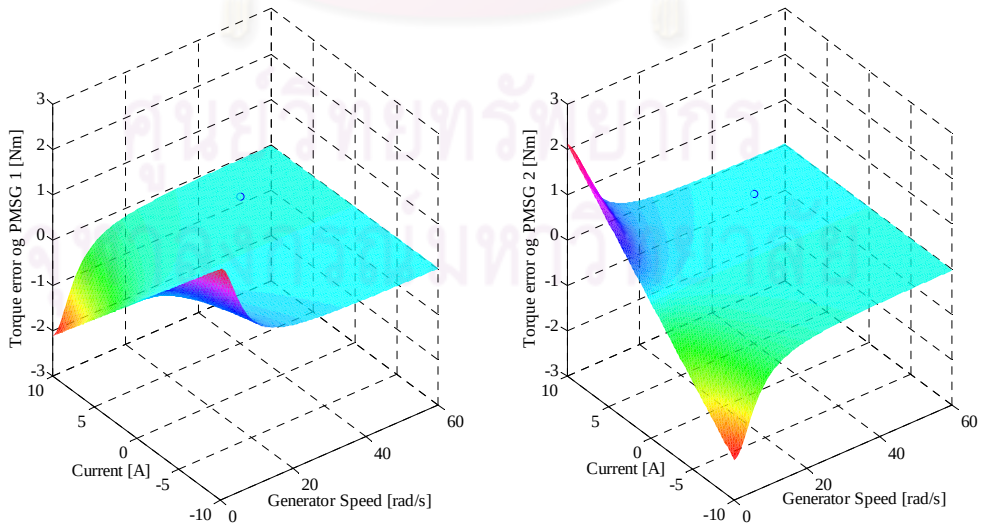

Fig. 4.8 Torque unbalance (ΔT_1 and ΔT_2) due to mismatched stator resistance ($R_1 = 10.34\ \Omega$ and $R_2 = 8.46\ \Omega$).

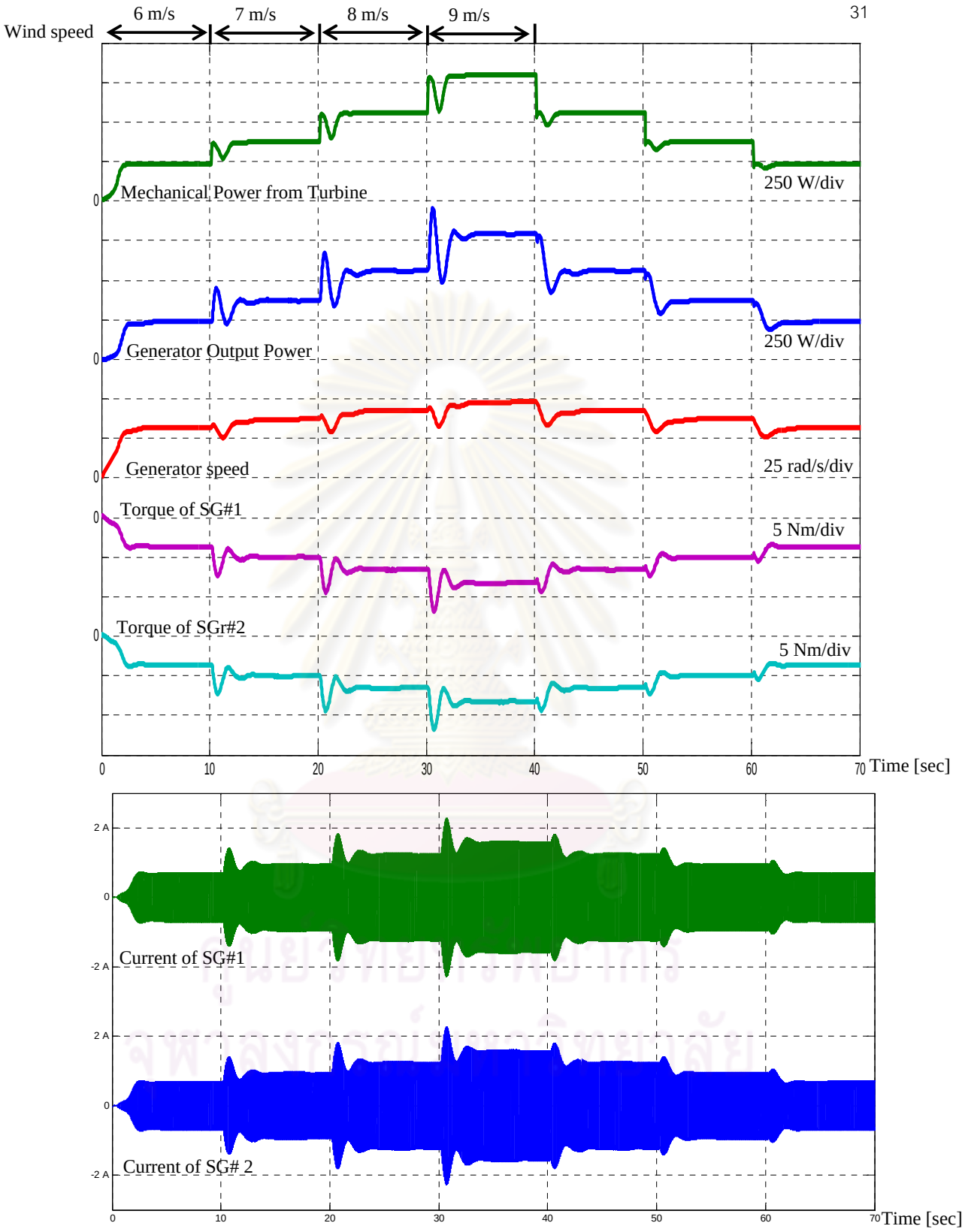

Fig. 4.9 Simulation results showing the performance of WECS with mismatched stator resistance.

The above results show that the mismatch of stator resistance has only the effect on the torque unbalance; (4.6)-(4.7), while the total torque controllability is not affected; (4.8); this is due to the cancellation of torque error among two generators. Fig. 4.8 indicates the torque unbalance caused by ±10% stator resistance mismatch, it is seen that only very low-speed region is sensitive to this resistance mismatch. In addition, Fig. 4.9 shows that the overall performance of WECS is well acceptable which means the tandem generators drive is robust to the mismatched stator resistance.

4.3 Effects of Mismatched Stator Inductance ΔL.

The current difference $\Delta\vec{i}$ that caused by the mismatch of stator inductance can be simply derived as:

$$\Delta\vec{i} = \frac{(L_2 - L_1)(sI + \omega J)}{2R \cdot I + (sI + \omega J)(L_1 + L_2)} \cdot \vec{i} \qquad (4.9)$$

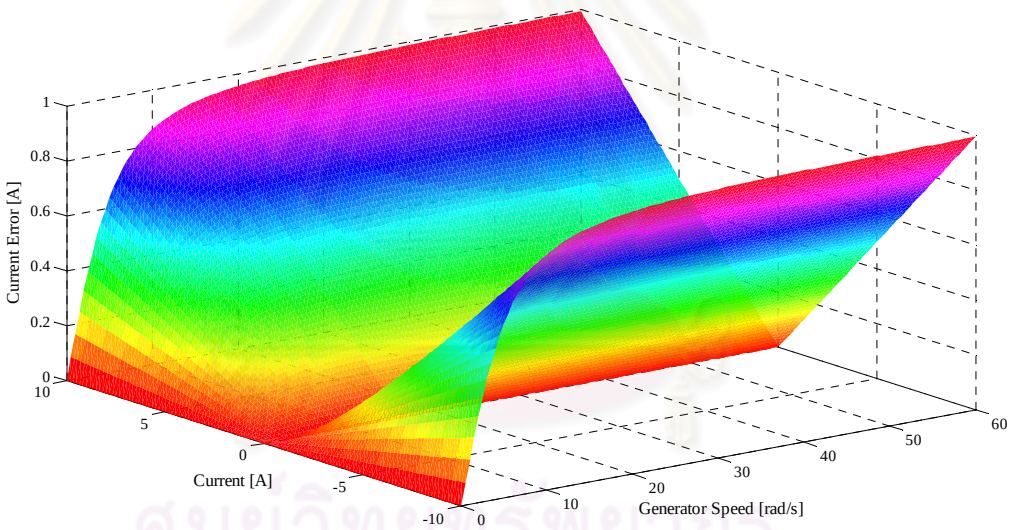

Fig. 4.10 Current difference $\left|\Delta\vec{i}\right|$ due to mismatched stator inductance, $L_1 = 0.0715\ H$ and $L_2 = 0.0585\ H$ (±10% of L).

From (4.9), the current difference can be illustrated in Fig. 4.10 and it is seen that the current difference is greater in higher speed range. The conceptual vector diagram for this case is similar to the one shown in Fig. 4.6. In the same manner as that of the mismatch of stator resistance, only the torque unbalance occurs ((4.6)-(4.7)) and there is no effect on the total torque controllability (4.8). The results from deviation of ±10% stator inductance are given in Fig. 4.11, in contrast to the case of stator resistance, the torque unbalance is more sensible in the high-speed region. The simulation results of WECS in Fig. 4.12 also clearly demonstrate the torque unbalance in high-speed range when the mismatched stator inductance is taken into account.

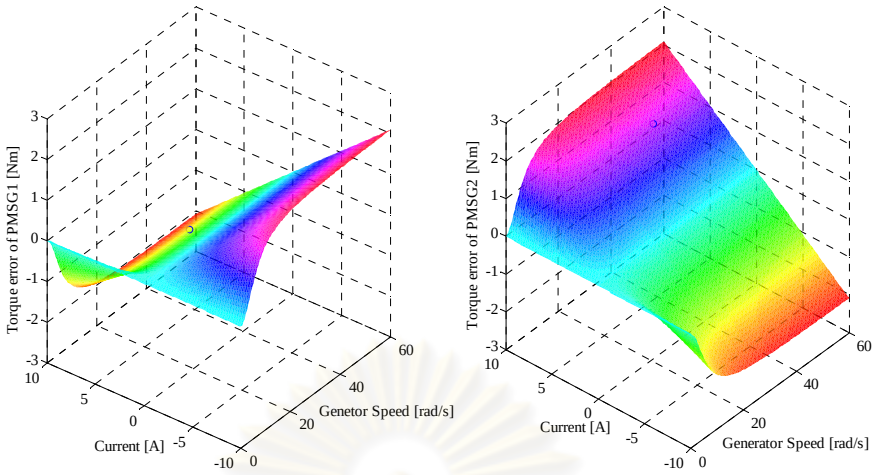

Fig. 4.11 Torque unbalance (ΔT_1 and ΔT_2) due to mismatched stator inductance; $L_1 = 0.0715\ H$ and $L_2 = 0.0585\ H$ (±10% of L .

ศูนย์วิทยทรัพยากร
จุฬาลงกรณ์มหาวิทยาลัย

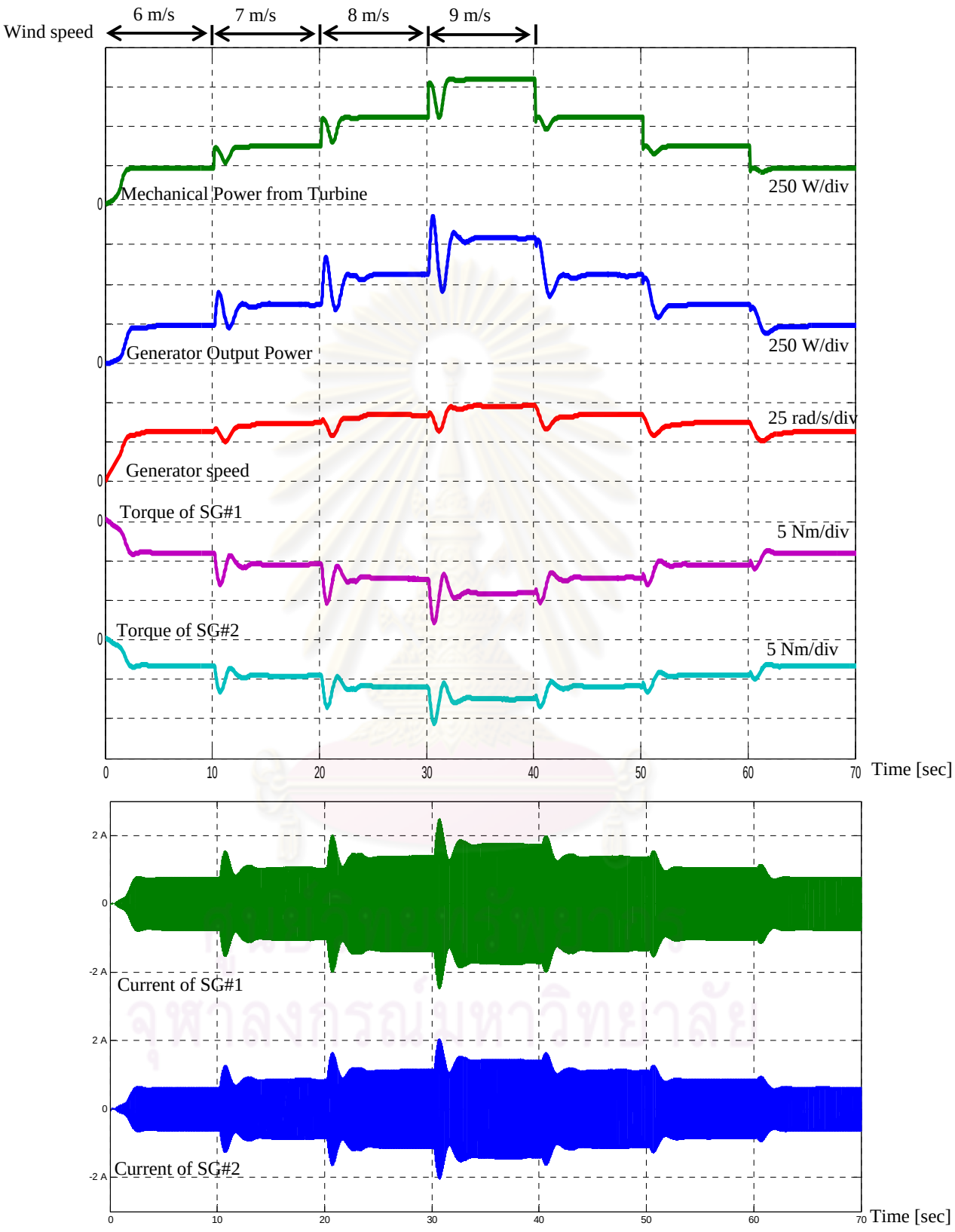

Fig. 4.12 Simulation results showing the performance of WECS with mismatched stator inductance.

4.4 Comparison of Effects of Mismatched Parameters

According to the sensitivity analysis in section 4.1-4.3, the effects of mismatched parameters can be concluded in Table 4.1. Among all mismatched parameter, the deviation of permanent magnet flux, especially the mismatched flux magnitude, causes the severe impact on both torque unbalance and torque controllability of the tandem generators drive. For the mismatched of stator resistance and inductance, there is no effect on total torque controllability, and the system is quite robust to the mismatched stator resistance.

Table 4.1 Comparisons of effects of mismatched parameters.

Mismatched parameter	Torque controllability degradation		Performance with mismatched parameter	
	Torque unbalance	Total torque error	Low speed	High speed
Flux position $\Delta\angle\vec{\psi}$	Yes	Yes	Fair	Fair
Flux magnitude $\Delta\lvert\psi\rvert$	Yes	Yes	Poor	Fair
Stator resistance ΔR	Yes	No	Fair	Good
Stator inductance ΔL	Yes	No	Good	Fair

ศูนย์วิทยทรัพยากร
จุฬาลงกรณ์มหาวิทยาลัย

CHAPTER V

IMPLEMENTATION AND EXPERIMENTAL RESULTS

5.1 Overall experiment setup.

Fig. 5.1 shows the experimental set up of wind energy conversion system; WECS, the main components of developed system are: 1) tandem synchronous generators; details are given in chapter 2, 2) MPPT scheme developed on TMS320F2812 platform, 3) back-to-back PWM converter and 4) wind turbine simulator.

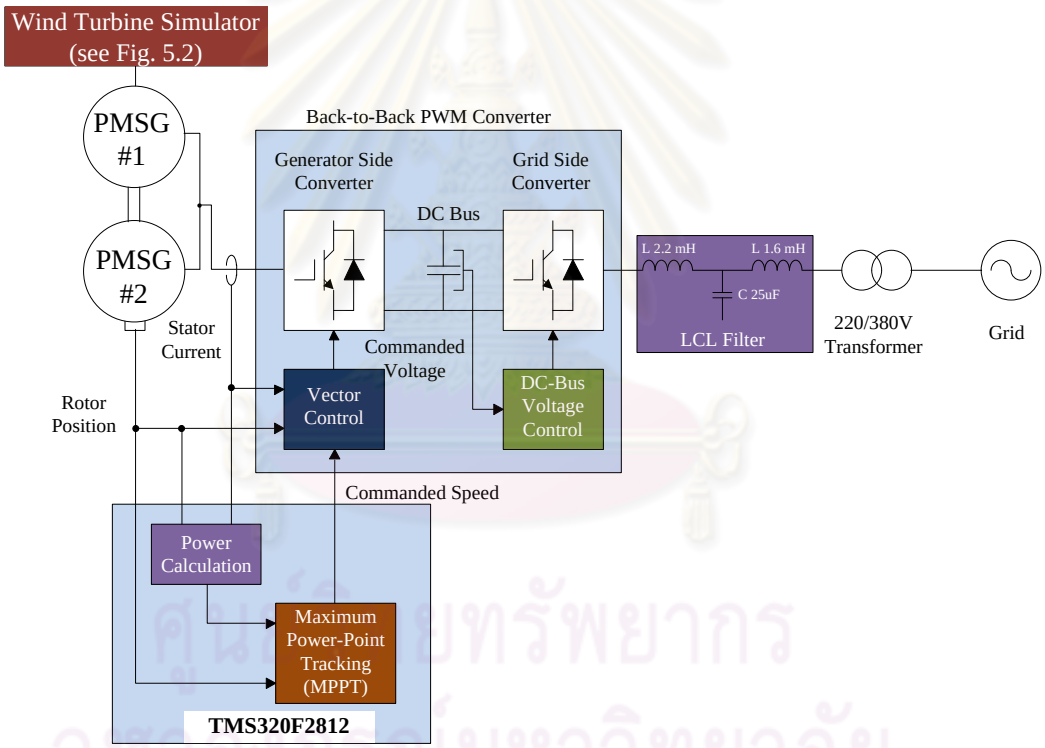

Fig. 5.1 Experiment setup of WECS

5.2 Back-to-Back PWM Converter.

As the wind turbine operates at variable speed according to available wind speed, the voltage generated is variable of magnitude and frequency. Therefore the power generated need to be processed before feeding to grid. This system uses the back-to-back PWM converter, which is used as linking between the generator side and grid. The PWM converter composes of two voltages-source inverters (VSI) and the capacitor which is connected in between them. The generator-side inverter is controlled by current-controlled vector control, and the grid side inverter is operated in 3-phase PWM rectifier mode with DC-Bus voltage regulation. The power flow can be bidirectional; either it can flow through the generator or through the grid. The LCL filter is also provided for the grid connection. Ratings of back-to-back PWM converter are listed in Table 5.1.

Table 5.1 Rating of back-to-back PWM converter.

Grid-side voltage:	3-phase AC, 220V, 50 Hz
Grid-side current:	8 A
Generator-side voltage:	3-phase AC, 0 – 220V, 0 – 600Hz
Generator-side current:	8 A

The function of generator-side converter is to track the maximum power at all available wind speeds. Therefore, the generator speed is controlled in order to follow the power-speed characteristics via the TMS320F2812 Digital Signal Processor. The TMS320F2812 is a single-board based which will receive current and position signals to calculate the commanded speed for generator-side converter.

5.3 Wind-Turbine Simulator.

5.3.1 Wind-turbine simulator by AC drive.

Wind turbine, in this thesis, is created by an AC drive as shown in Fig. 5.2; the AC drive is operated in torque control mode and it is coupled to the tandem synchronous generators through a torque transducer. As a commanded torque for AC servo inverter, the turbine's torque is calculated from power-speed characteristic of wind turbine as described in section 3.3.3. This calculation task is performed by another TMS320LF2047 Digital Signal Processor; the rotor position is detected for speed calculation, while the wind speed is assigned as an input. Table 5.2 is the ratings of AC servo drive used in this wind-turbine simulator.

Table 5.2 Ratings of AC servo drive

Motor	
Voltage:	3phase, 200V
Power:	3.0 kW, 20.6 A
Speed:	1500 rpm
Inverter	
Voltage input:	200V – 240V, 50/60 Hz
Voltage output:	0 – 240V, 0 – 600Hz
Power output:	3.7kW, 17 A

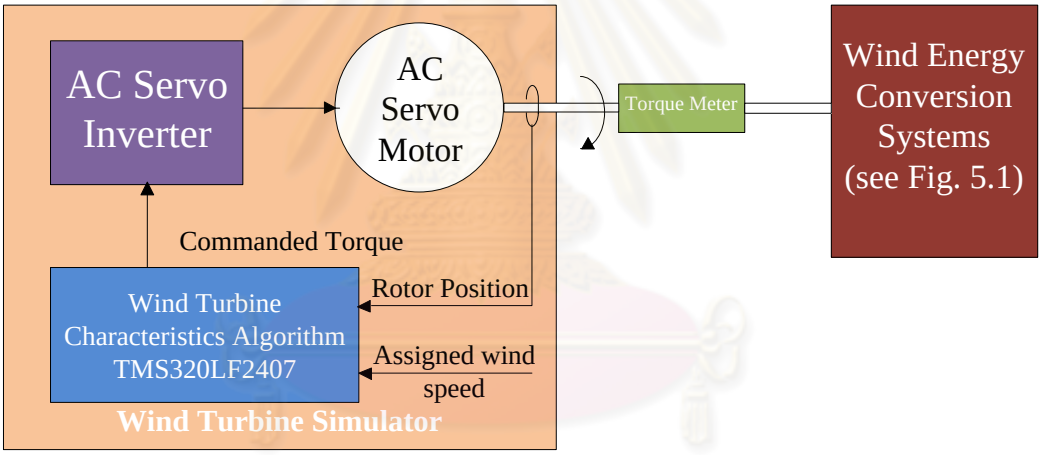

Fig. 5.2 Implementation of wind-turbine simulator.

5.3.2. Evaluations of wind-turbine simulator.

Fig. 5.3(a) is the characteristic of turbine's torque versus rotor speed which is derived from the power-speed characteristic of wind turbine. For any assigned wind speed 6-9 m/s, the turbine's torque in 5.3(a) is generated, from TMS320LF2407, as the commanded torque for AC servo drive. Performance of wind-turbine simulator is evaluated and carried out in Fig. 5.4(b); the shaft torque of servo drive is measured and the resultant torque-speed characteristic is plotted for each wind speed. It is seen in Fig. 5.4(b) that the AC servo drive can nicely produce the output torques corresponding to the characteristic of wind turbine (Fig. 5.4(a)) and it can be employed as a prime mover for the testing of WECS in the next sections.

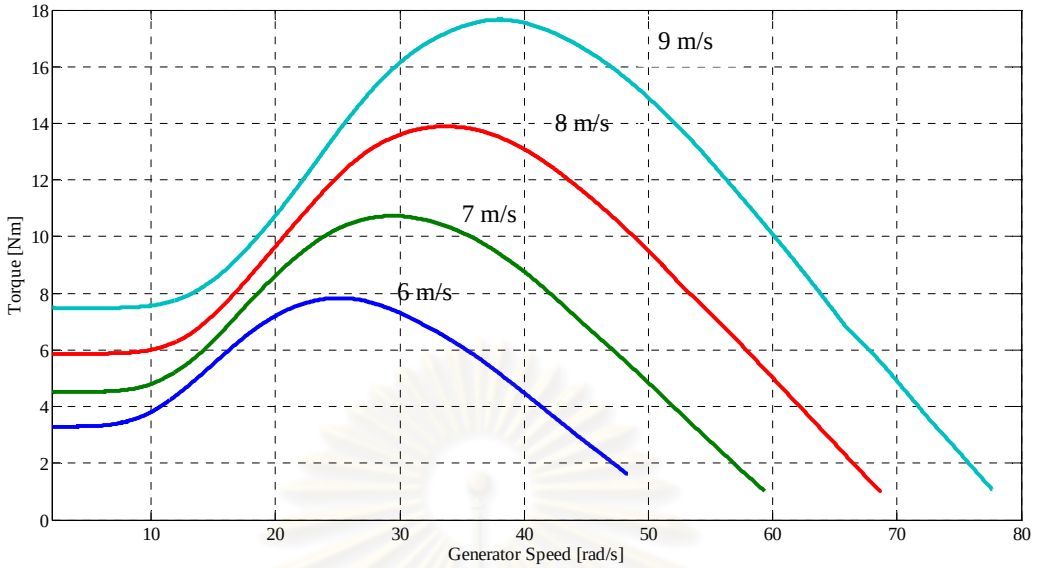

(a) Commanded torque-speed characteristic generated from TMS320LF2407

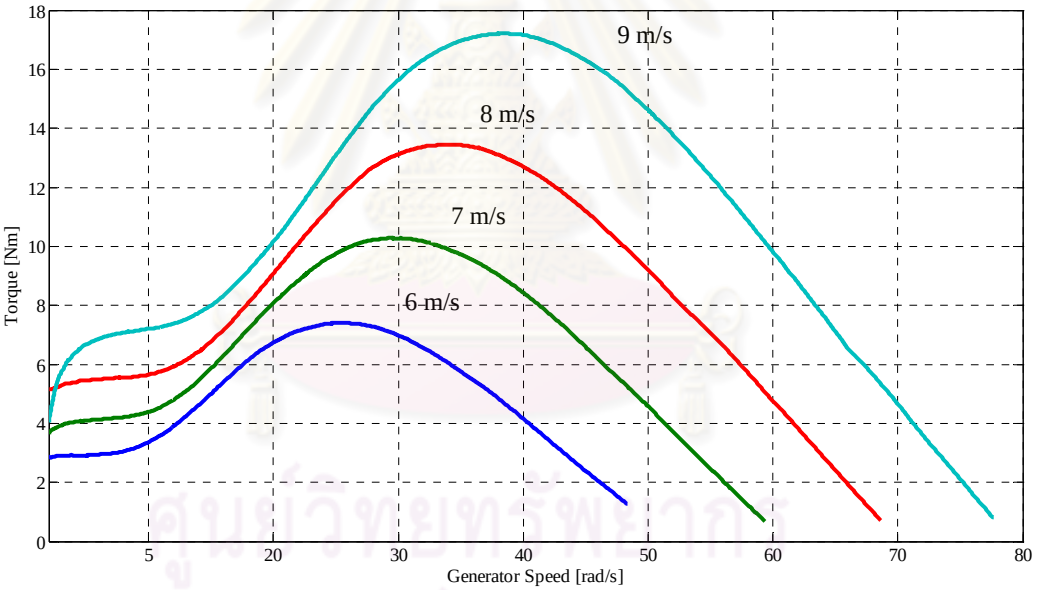

(b) Torque-speed characteristic of wind-turbine simulator (measured from torque meter)

Fig. 5.3 Evaluation of wind-turbine simulator.

5.4 Experimental Results of WECS with Tandem Synchronous Generators

Regarding the experiment set up and wind-turbine simulator in previous sections, the performances of WECS with tandem synchronous generators are tested by means of following investigations.

- Performance of MPPT.
- Power gathering and current sharing of tandem generators.
- Effects of mismatched flux position.

5.4.1 Performance of MPPT

In Fig. 5.4, the wind speed is varied continuously and slowly, the MPPT scheme can effectively track the maximum power for each wind speed. The responses against sudden change of wind speed are depicted in Figs. 5.5-5.7. Generators' torque can be properly controlled during the sudden change of wind speed. The MPPT can successfully track the maximum power point according to each wind speed with acceptable rate of convergence.

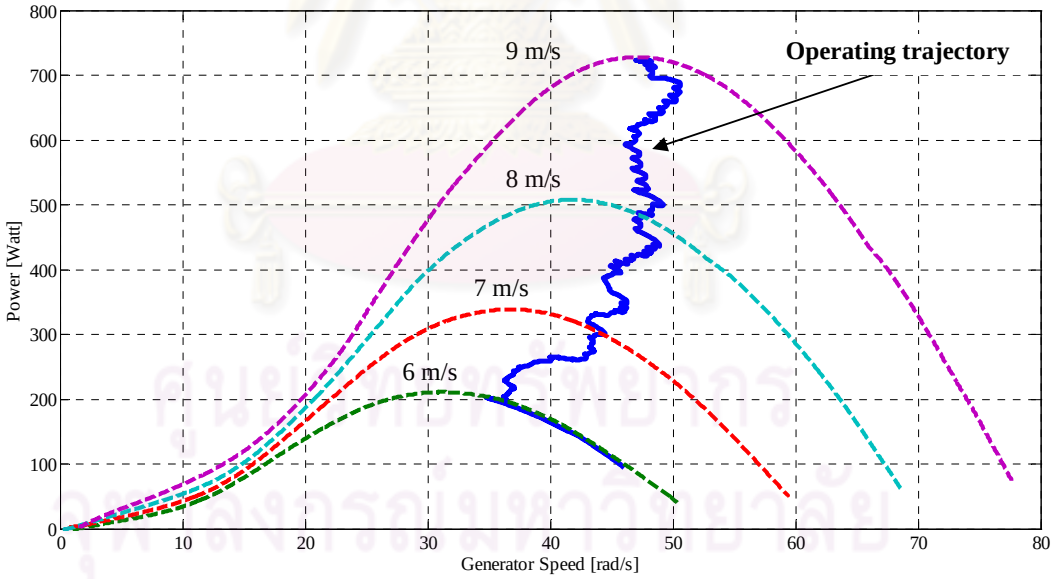

Fig. 5.4 Performance of MPPT on power-speed plane when wind speed is varied slowly.

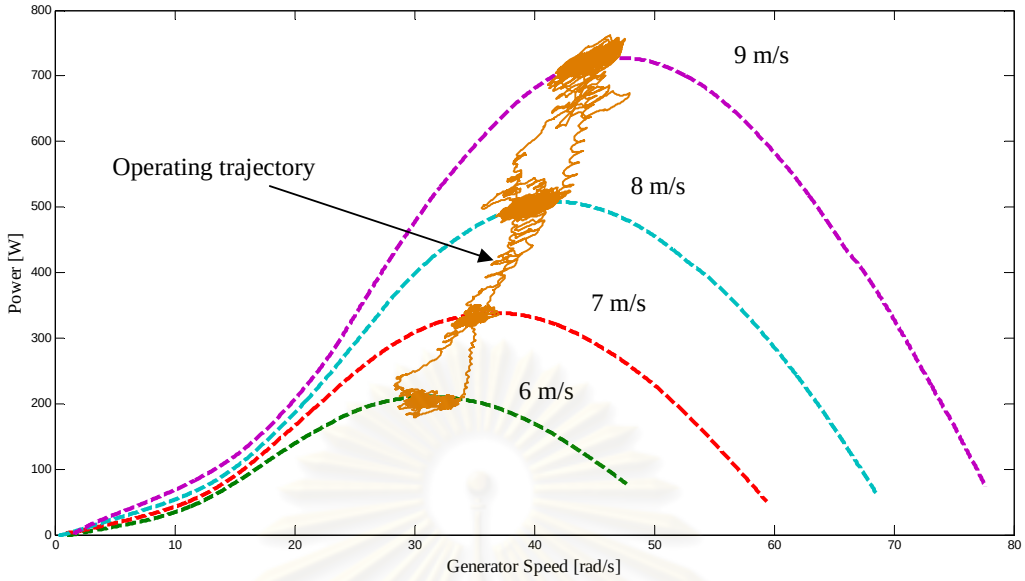

Fig. 5.5 Performance of MPPT on power-speed plane when wind speed is suddenly changed.

5.4.2 Power gathering and current sharing of tandem generators

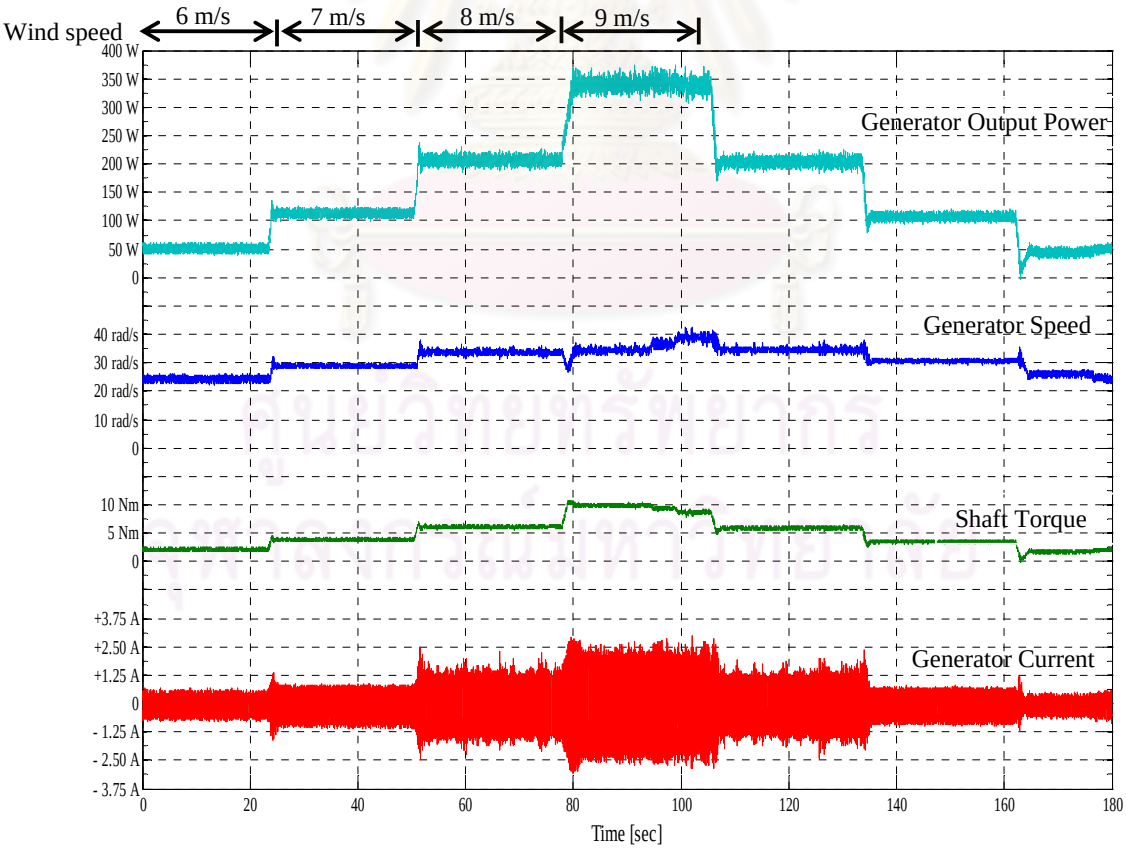

Fig. 5.6 Performance of MPPT with single synchronous generators when wind speed is suddenly changed.

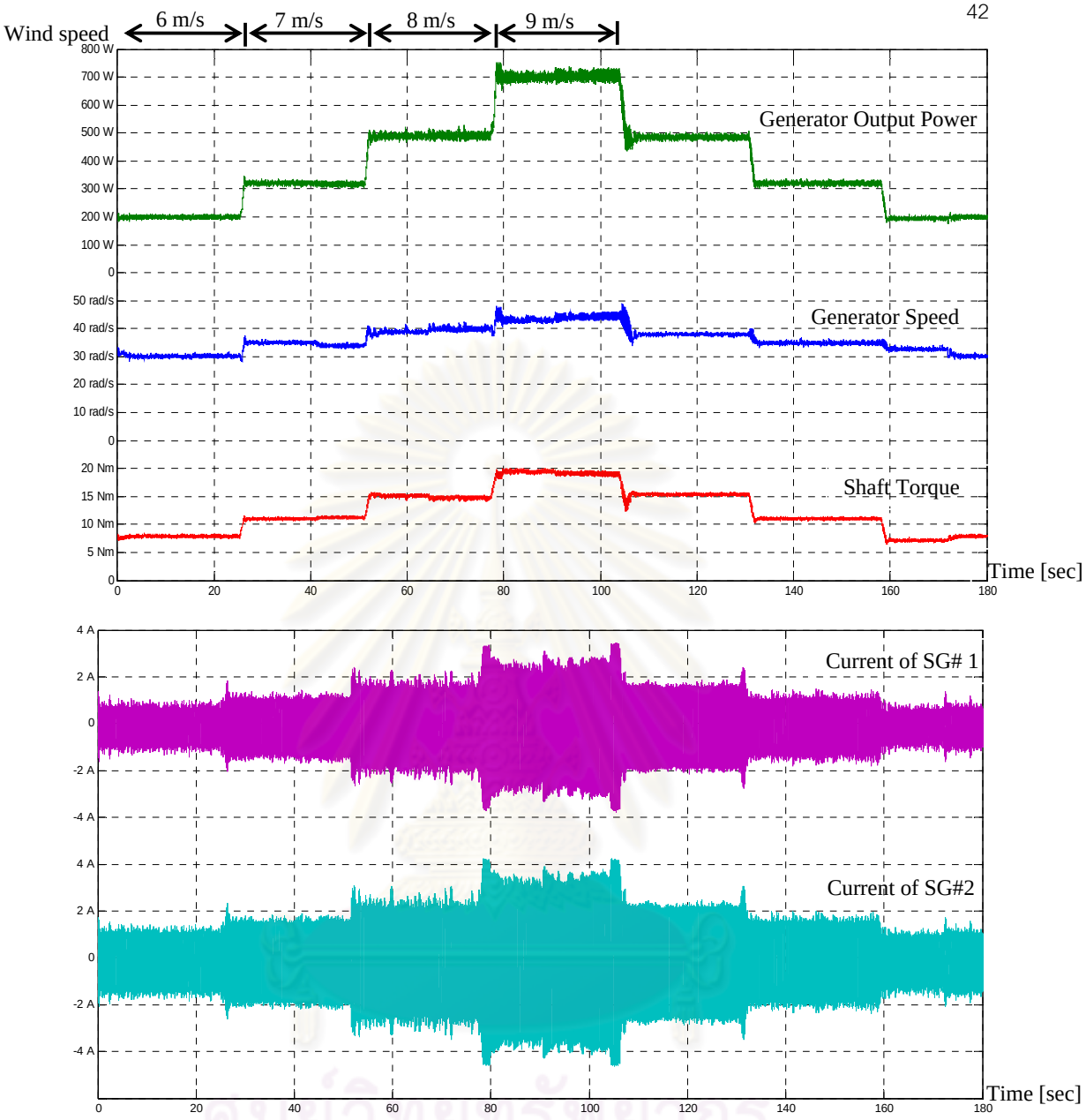

Fig. 5.7 Performance of MPPT with tandem generators when wind speed is suddenly changed.

In order to demonstrate power gathering; which is the main advantage of tandem generators, Figs 5.6 and 5.7 are given. The tandem generators shown in Fig. 5.7 can produce roughly twice the output power from single generator, as shown in Fig. 5.6. Concerning current sharing, each generator's current in, Fig. 5.7, is considered. The currents are quite balance at low speed with low torque (at 6 m/s of wind speed), however the unbalance can be clearly observed at higher speed with higher torque (at higher wind speed, i.e. 8m/s - 9 m/s). This is caused by the mismatched of flux position which will be investigated in section 5.4.3. Experimental

result in Fig. 5.8 is given, in addition, to show that the back-to-back converter successfully feeds the electrical power into the grid. It can be concluded that, the overall performance of WECS with tandem generators is satisfactory and it is feasible to employ this concept in practice.

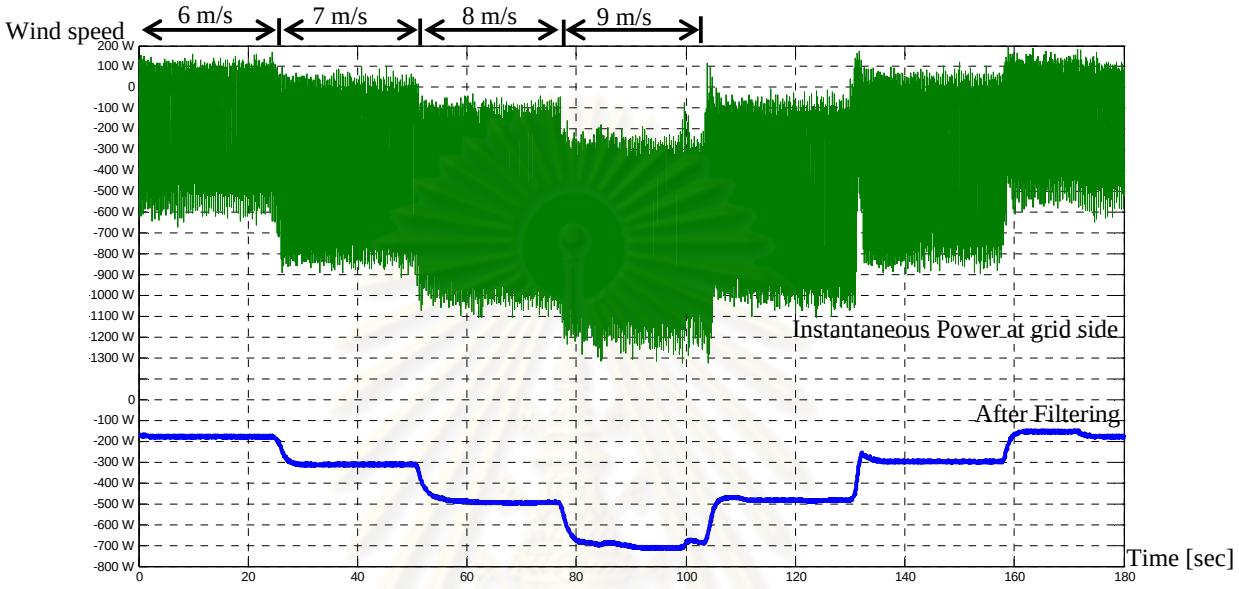

Fig. 5.8 Power at grid side.

5.4.3 Effects of mismatched flux position

Among all parameters of generators, the mismatched flux position is easily occurred in practice; since generators are multi-pole type, a high accuracy is required for the alignment of permanent-magnet poles of tandem generators. In order to investigate the alignment of permanent-magnet poles, the open circuit test is setup and the back EMF waveforms of generators are measured as shown in Fig. 5.9. The back EMF waveforms reflect the mismatched flux position for about 10^{o} (electrical degree) and it can cause the unbalance of current especially in high-speed range as depicted in the experimental results in Figs. 5.7 and 5.10, and this is also confirmed by the simulation result in Fig. 5.11.

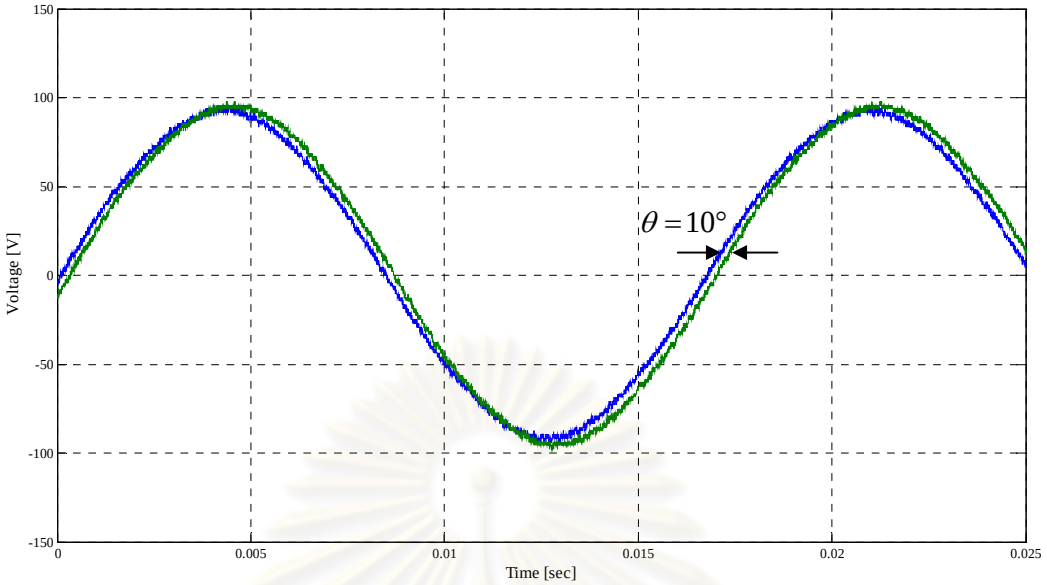

Fig. 5.9 Back EMF waveforms of tandem synchronous generators.

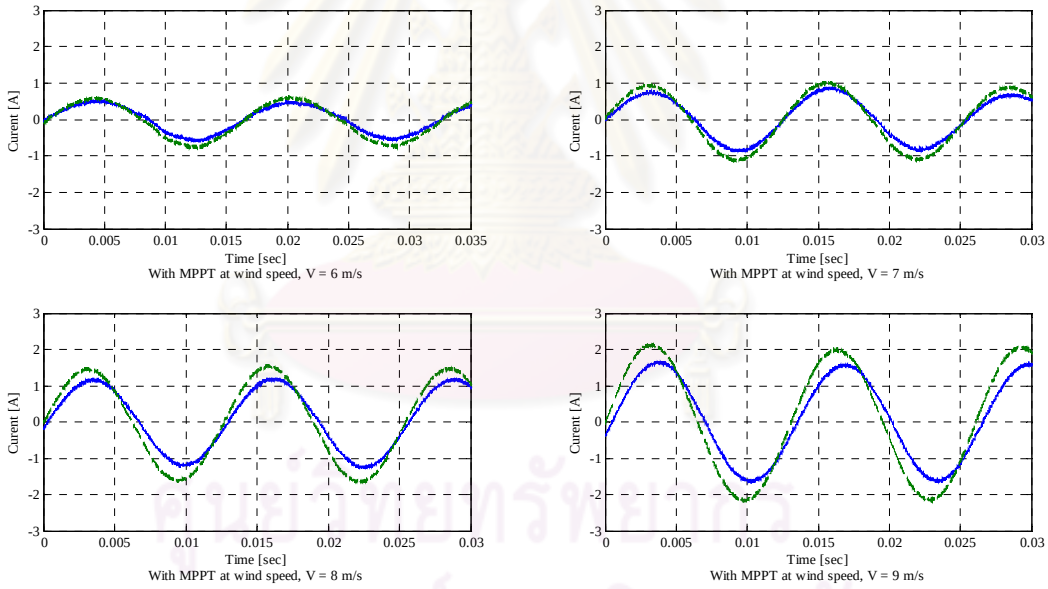

Fig. 5.10 Experimental results showing current unbalance due to the effect of mismatched flux position ($\Delta\measuredangle\vec{\psi} = 10°$)

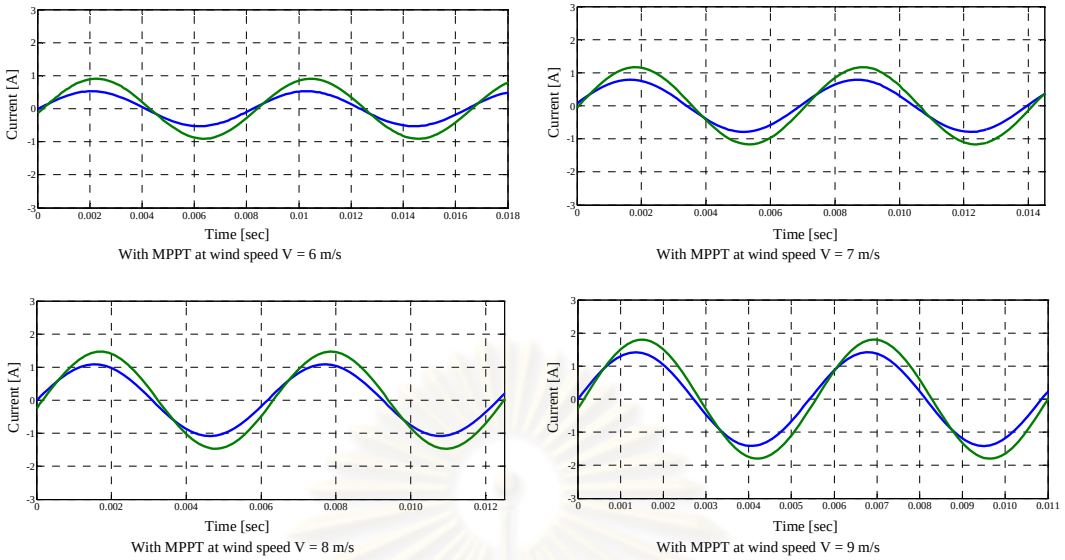

Fig. 5.11 Simulation results showing current unbalance due to the effect of mismatched flux position ($\Delta\measuredangle\vec{\psi} = 10°$)

ศูนย์วิทยทรัพยากร
จุฬาลงกรณ์มหาวิทยาลัย

CHAPTER VI
CONCLUSIONS

6.1 Significant outcomes.

In this thesis, the significant outcomes are listed as follows:

- The concept of tandem generators is proposed for the direct drive of multiple multi-pole permanent magnet synchronous generators (PMSG) for wind energy conversion systems (WECS).
- Vector control and MPPT scheme are employed to control the generators' torques and to gain the maximum power from wind turbine.
- Effects of mismatched parameters of generators are analyzed and it is revealed that among all mismatched parameters, the effect of mismatched flux is considerable.
- The validity of proposed concept and analysis results are verified by simulation and experimental setup.

6.2 Future works

The direct drive of tandem synchronous generators is the alternative concept for WECS. Some issues are still left for the future work, i.e.

- Comparing the parallel-connected tandem generators with the series-connected topology.
- Using three or more generators in tandem.
- Design guideline for the PI controller of MPPT scheme.

ศูนย์วิทยทรัพยากร
จุฬาลงกรณ์มหาวิทยาลัย

REFERENCES

[1] Matsumoto, Y.; Ozaki, S. and Kawamura, A. “A Novel Vector Control of Single - inverter-multiple-induction-motors Drives for Shinkansen Traction System”. Power Electronics Conference and Exposition, 2001. APEC 2001 Page(s): 608 – 614 vol. 1.

[2] Kelecy, P. M. and Lorenz, R. D.; “ Control Methodology for Single Inverter, Parallel Connected Dual Induction Motor Drives for Electric Vehicles”. Power Electronics Specialists Conference, PESC 1994 Page(s): 987 – 991 vol. 2.

[3] Matsuse, K.; Kawai, H.; Kouno, Y. and Oikawa, J.; “Characteristics of Speed Sensorless Vector Controlled Dual Induction Motor Drive Connected in Parallel Fed by a Single Invert”. Industry Application, IEEE Transactions on Volume: 40. Year: 2004 Page(s): 153 – 161.

[4] Taniguchi, M.; Yoshinaga, T. and Matsuse, M.; “A Speed-Sensorless Vector of Parallel-Connected Multiple Induction Motor Drives with Adaptive Rotor Flux Observers”. Power Electronics Specialists Conference, PESC 2006. Page(s): 1-5.

[5] S. Sangwongwanich, et. al., “A Unified Speed Estimation Design Framework for Sensorless AC Motor Drives Based on Positive-Real Property”. Power Conversion Conference-Nagoya, 2007. PCC ’07. 2-5 April 2007 Page(s):1111-1118.

[6] M. Chinchilla, et. al., “Control of Permanent-Magnet Generator Applied to Variable-Speed Wind-Energy Systems Connected to the Grid”.IEEE Transaction on Energy Conversion, vol 21, no. 1, March 2006. Page(s):130-135.

[7] R. K. Sharma, et. al., “Vector control of a PMSM”. India Conference, 2008. INCICON 2008. Annual IEEE. Vol. 1, Page(s); 81 -86, 11-13 Dec. 2008.

[8] P. Chanthavong, S. Suwankawin, and H. Akagi, “A direct drive of multiple multi-pole synchronous generators for wind energy conversion system”. ECTI-CON 2010, Page(s): 1021 – 1025, 19-21 May 2010.

[9] Frede Blaabjerg and Zhe Chen. **Power Electronics for Modern Wind Turbine.** The Morgan and Claypool Publishers’ series. 2006.

[10] M. Iulian, I. B. Antoneta, C. Nicolaos-Antonio, and C. Emil. **Optimal Control of Wind Energy Systems.** Springer-Verlag London Limited. Springer. 2008.

[11] D. B. Fernando, H. De Battista, and J. M. Ricardo. **Wind Turbine Control Systems.** Springer-Verlag London Limited. Springer. 2007.

[12] F. Brenden, F. Damian, B. Leslie, J. Nick, M. David, O. Mark, W. Rechard, and A. L. Olimpo. **Wind Power Integration, Connection and system operational aspects**. The Institution of Engineering and Technology, London, United Kingdom, 2007

APPENDIX

ศูนย์วิทยทรัพยากร
จุฬาลงกรณ์มหาวิทยาลัย

APPENDIX

1 Hardware of Wind Energy Conversion Systems

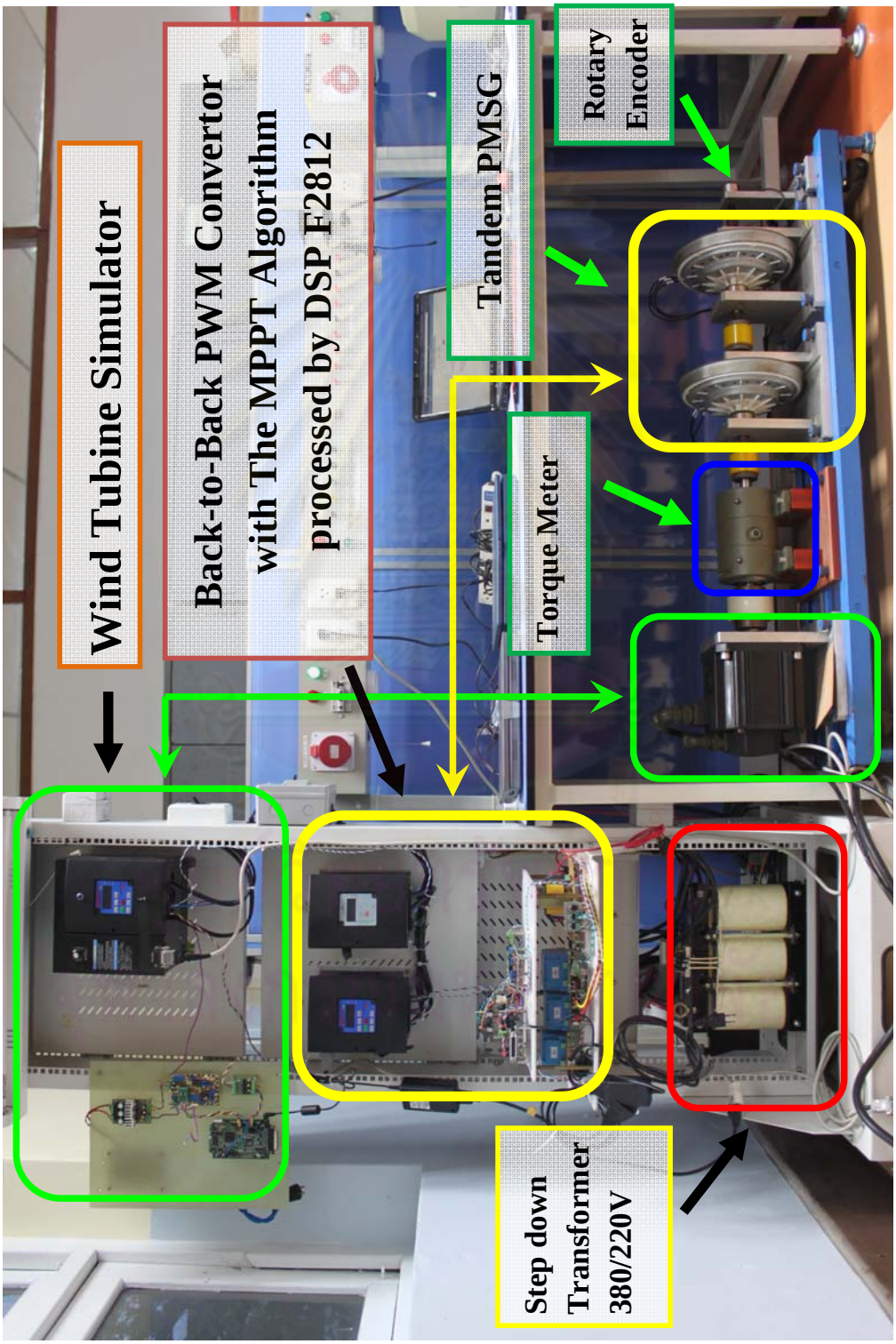

2 MPPT Algorithm processed by DSP F2812

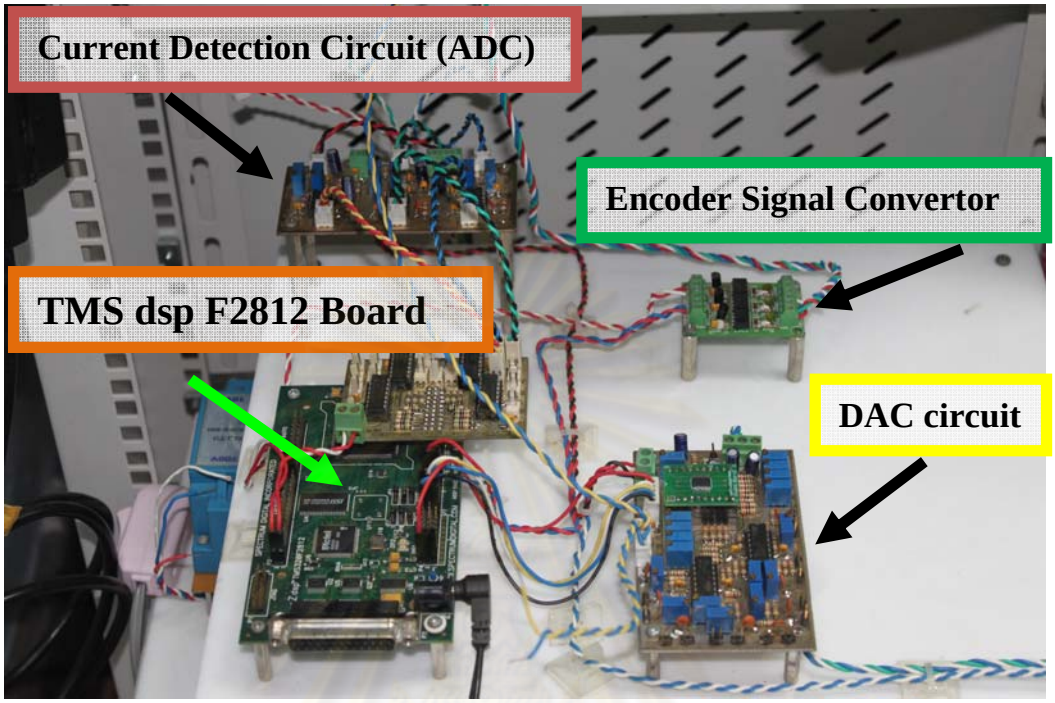

ศูนย์วิทยทรัพยากร
จุฬาลงกรณ์มหาวิทยาลัย

BIOGRAPHY

Phanxay Chanthavong was born on April, 07 1985 in Vientiane, the capital city of Lao P.D.R. He spent most of his time in Viantiane from the primary school until he finished his undergraduate study. He studied in Department of Electrical Engineering, major of Electrical Engineering, National University of Laos (NUoL), Vientaine, Lao P.D.R. He earned his Bachelor of Engineering degree in 2006. He was awarded AUN/SEED-Net scholarship to continue his study in Department of Electrical Engineering, Faculty of Engineering, Chulalongkorn University, Bangkok, Thailand in June 2008. His current research interests are in the renewable energy and electric drive in machine.

ศูนย์วิทยทรัพยากร
จุฬาลงกรณ์มหาวิทยาลัย